Tectonophysics 863 (2023) 229976

Contents lists available at ScienceDirect

Tectonophysics

journal homepage: www.elsevier.com/locate/tecto

Quality-assurance of heat-flow data: The new structure and evaluation scheme of the IHFC Global Heat Flow Database

Sven Fuchs [a], Ben Norden [a,*], Florian Neumann [a], Norbert Kaul [b], Akiko Tanaka [c], Ilmo T. Kukkonen [d], Christophe Pascal [e], Rodolfo Christiansen [e], Gianluca Gola [f], Jan Šafanda [g], Orlando Miguel Espinoza-Ojeda [h], Ignacio Marzan [i], Ladislaus Rybach [j], Elif Balkan-Pazvantoğlu [k], Elsa Cristina Ramalho [l], Petr Dědeček [g], Raquel Negrete-Aranda [m], Niels Balling [n], Jeffrey Poort [o], Yibo Wang [p], Argo Jõeleht [q], Dušan Rajver [r], Xiang Gao [s], Shaowen Liu [t], Robert Harris [u], Maria Richards [v], Sandra McLaren [w], Paolo Chiozzi [x], Jeffrey Nunn [y], Mazlan Madon [z], Graeme Beardsmore [w], Rob Funnell [aa], Helmut Duerrast [ab], Samuel Jennings [a], Kirsten Elger [a], Cristina Pauselli [ac], Massimo Verdoya [ad]

[a] *Helmholtz Centre Potsdam German Research Centre for Geoscience GFZ, Potsdam, Germany*
[b] *University of Bremen, Geowissenschaften, Bremen, Germany*
[c] *Geological Survey of Japan, National Institute of Advanced Industrial Science and Technology, Tsukuba, Japan*
[d] *Dept. of Geosciences and Geography, University of Helsinki, Finland*
[e] *Institute of Geology, Mineralogy and Geophysics, Ruhr University Bochum, Germany*
[f] *Institute of Geosciences and Earth Resources, National Research Council, Turin, Italy*
[g] *Institute of Geophysics, Czech Academy of Sciences, Prague, Czechia*
[h] *CONAHCYT - Instituto de Investigaciones en Ciencias de la Tierra, Universidad Michoacana de San Nicolás de Hidalgo, Morelia, Mexico*
[i] *Geological and Mining Institute of Spain IGME-CSIC, Spain*
[j] *Institute of Geophysics ETHZ, Zurich, Switzerland*
[k] *Dokuz Eylül University, Department of Geophysical Engineering, İzmir, Turkey*
[l] *Laboratório Nacional de Energia e Geologia, Portugal*
[m] *CONAHCYT, Departamento de Geología, División de Ciencias de la Tierra, Centro de Investigación Científica y Educación Superior de Ensenada (CICESE), Mexico*
[n] *Department of Geoscience, Aarhus University, Aarhus, Denmark*
[o] *Sorbonne Université, CNRS, Institut des Sciences de la Terre de Paris, Paris, France*
[p] *Institute of Geology and Geophysics Chinese Academy of Sciences, Beijing, China*
[q] *Department of Geology, University of Tartu, Estonia*
[r] *Geological Survey of Slovenia, Ljubljana, Slovenia*
[s] *Institute of Oceanology, Chinese Academy of Sciences, Qingdao, China*
[t] *School of Geography and Ocean Science, Nanjing University, China*
[u] *Oregon State University, USA*
[v] *SMU Geothermal Laboratory, Dallas, TX, USA*
[w] *School of Geography, Earth and Atmospheric Sciences, University of Melbourne, Australia*
[x] *Department of Earth, Environment and Life Sciences, University of Genoa, Italy*
[y] *Chevron Technical Center, Houston, TX, USA*
[z] *Continental Shelf Project, National Security Council, Malaysia*
[aa] *GNS Science, New Zealand*
[ab] *Geophysics, Faculty of Science, Prince of Songkla University, Hat Yai,Thailand*
[ac] *Dipartimento di Fisica e Geologia, University of Perugia, Italy*
[ad] *Dept. of Earth, Environment and Life Sciences (DISTAV), University of Genoa, Italy*

ARTICLE INFO

Keywords:
Heat-flow density
Quality scheme

ABSTRACT

Since 1963, the International Heat Flow Commission has been fostering the compilation of the Global Heat Flow Database to provide reliable heat-flow data. Over time, techniques and methodologies evolved, calling for a reorganization of the database structure and for a reassessment of stored heat-flow data. Here, we provide the

* Corresponding author.
E-mail address: ben.norden@gfz-potsdam.de (B. Norden).

https://doi.org/10.1016/j.tecto.2023.229976
Received 26 February 2023; Received in revised form 8 June 2023; Accepted 21 June 2023
Available online 4 July 2023

Thermal geophysics
Global heat flow database (GHFD)
Thermal parameter
Data information system
International Heat Flow Commission (IHFC)

results of a collaborative, community-driven approach to set-up a new, quality-approved global heat-flow database. We present background information on how heat-flow is determined and how this important thermal parameter could be systematically evaluated. The latter requires appropriate documentation of metadata to allow the application of a consistent evaluation scheme. The knowledge of basic data (name and coordinates of the site, depth range of temperature measurements, etc.), details on temperature and thermal-conductivity data and possible perturbing effects need to be given. The proposed heat-flow quality evaluation scheme can discriminate between different quality aspects affecting heat flow: numerical uncertainties, methodological uncertainties, and environmental effects. The resulting quality codes allow the evaluation of every stored heat-flow data entry. If mandatory basic data are missing, the entry is marked accordingly. In cases where more than one heat-flow determination is presented for one specific site, and all of them are considered for the site, the poorest evaluation score is inherited to the site level. The required data and the proposed scheme are presented in this paper. Due to the requirements of the newly developed evaluation scheme, the database structure as presented in 2021 has been updated and is available in the appendix of this paper. The new quality scheme will allow a comprehensible evaluation of the stored heat-flow data for the first time.

1. Introduction

The Earth's internal heat is the sum of various sources: natural radiation of Earth's constituent heat producing elements, remaining heat from the planet formation, exothermic chemical reactions, and kinetic friction due to gravitation and differential rotation movements. The heat-flow density (HFD) – often termed the terrestrial surface heat flow, heat flux or geothermal flow – quantifies the amount of thermal energy that the Earth loses per unit surface area and time. Variations in surface heat flow provide fundamental insights on the thermal regime and, coupled with other geodata, constraints on the evolution and geodynamics of the crust and lithosphere (e.g., Čermák and Rybach, 1979; Davies and Davies, 2010; Davies, 2013; Mareschal and Jaupart, 2013; Lucazeau, 2019). Heat-flow data contribute to our understanding of large-scale geodynamic processes such as plate tectonics (e.g., Polyak and Khutorskoy, 2018), the fundamental planetary energy balance (e.g., Chapman and Rybach, 1985; Clauser, 2006), local and regional processes such as neotectonic activity (e.g., Carlino, 2018; Jiang et al., 2019), fluid flow (e.g., Alföldi et al., 1985; Le Gal et al., 2018; Harris et al., 2020) or mineralization (e.g., Houseman et al., 1989), the selection and location of geothermal energy projects (e.g., Bédard et al., 2017), and the geological record of past land surface temperature changes (e.g., Wang and Lewis, 1992; Huang et al., 2000; Harris and Chapman, 2001; Bodri and Cermak, 2007; Gosnold and Njoku, 2017).

The total rate at which the Earth is currently losing heat is estimated in the range of 44–47 TW (Davies, 2013; Furlong and Chapman, 2013). But, in detail, the surface HFD (given in mW/m^2) varies considerably between locations. Interpreting and understanding the global, regional and local thermal field requires in-depth knowledge of thermo-physical parameters and thermal processes. Unlike many other geophysical data, the collection of surface HFD is complicated by the need for temperature (T) data from boreholes, laboratory measurements of thermal conductivity (TC) as well as a detailed knowledge of local geological and geophysical data. Moreover, direct measurements of in-situ rock temperatures and thermo-physical rock properties are restricted to drillable depths of the sub-surface and perturbing thermal effects related to near-surface phenomena or artificial thermal disturbances caused by drilling processes may overprint the equilibrium thermal field and affect HFD determinations.

The study of the Earth's temperature field has a long history. Obvious thermal manifestations like hot springs, volcanoes and temperatures encountered during early mining activities made it evident that the Earth's interior is hot and that there is an increase in temperature with depth. More systematically, temperature-depth and HFD data have been acquired around the world since the 1930s. However, the distribution of observations has remained highly uneven. Continental data mainly reflect the locations of boreholes associated with mining, hydrocarbon exploration and other (exploitation) activities. In contrast, marine heat-flow probes constructed for rapid observations at sea have allowed heat-flow data to be obtained in major offshore surveys for relatively little marginal cost.

The International Heat Flow Commission (IHFC, www.ihfc-iugg.org) focuses on the HFD determination and documentation. IHFC is a commission of the International Association of Seismology and Physics of the Earth's Interior (IASPEI) with the objective of discussing advances and opportunities from heat-flow research, to support geothermal researchers and to promote all aspects of geothermal research to the wider geoscientific community. The International Association of Volcanology and Chemistry of the Earth's Interior (IAVCEI) and the International Association of the Physical Sciences of the Ocean (IASPO) of the International Union of Geodesy and Geophysics (IUGG) are co-founding associations and participate in the activities of the commission. The first global compilation of HFD determinations was carried out by Birch (1954) and contained 63 heat-flow values. Over the next few decades, heat-flow data were simply used, or combined with a variety of geophysical and geological methods in an attempt to reveal global and continental heat-flow distribution characteristics (e.g., Chapman and Pollack, 1975; Sass and Lachenbruch, 1979; Pollack, 1982; Čermák and Rybach, 1991; Shapiro and Ritzwoller, 2004). Since 1963, the IHFC has been fostering the compilation of the Global Heat Flow Database (GHFD) to provide reliable heat-flow data. Reflecting the needs and technical capabilities at each respective time, the IHFC has released several data publications during its lifetime (e.g., Lee, 1963; Lee and Uyeda, 1965; Lee and Clark, 1966; Simmons and Horai, 1968; Jessop et al., 1976; Haenel et al., 1988; Global Heat Flow Compilation Group, 2013). More recently and beyond the IHFC framework, Hasterok (2019) and Lucazeau (2019) published heat-flow data compilations based on the GHFD.

To meet the requirements for a thorough evaluation of the global heat flow database, Jessop et al. (1976) were the first to provide a data quality evaluation scheme based on their database structure and the compilation of the World Heat Flow Data Collection available at that time. In their contribution, Jessop et al. proposed that individual users should make their own quality judgment based on the information available for each location, including:

1. the depth interval of measurement
2. the amount of data used to determine heat flow; and
3. any apparent variations in heat flow where multiple determinations were reported over short lateral distances

Jessop et al. (1976) introduced one specific additional parameter termed "consistency". This parameter was particularly suited for shallow (marine) temperature-probe measurements, but it was also applied to other HFD data. Based on previous temperature-probe data of the Lamont-Doherty Geological Observatory, consistency was classified using a 5-level rating scale (A to E) based on the estimation of vertical variability, probe tilt and uncertainty in the conductivity measurement (A: heat-flow variation of <10%, B: variation of 10–20%, C: variation >20%, D: probe tilt not determined, and E: variation indeterminable).

Although this quality scheme in the first instance provided some information on the accuracy of the HFD measurement itself, it did not provide detailed information on the reliability nor gave information on the applied technologies. Jessop et al. (1976) acknowledged that poor measurement techniques, lack of environmental corrections and other factors imposed limitations on the applicability of their quality scheme. More recently, Lucazeau (2019) took advantage of this classification in his personal version of the GHFD allowing an improved application of the evaluation for both probe sensing and borehole data. He uses five classes depending on the variation of heat flow with depth: class A (very good, with a variation of <10%), class B (good, with a variation of <20%), class C (average, with a variation of <30%), class D (data not used in heat-flow maps, variation is >30%), and class Z (variation not specified).

In principle, quality judgment by the user could also make use of further codes or metadata fields available in the published databases. However, this possibility has been severely hampered by the limited amount of metadata that has generally been provided, and hence available in the existing global database, for legacy heat flow determinations. Moreover, users needed to make their individual assessment of the quality of data used, based on their particular application or research question.

In 2020, the IHFC initiated an international project to review the GHFD (the *Global Heat Flow Data Assessment* project; http://assessment.ihfc-iugg.org) and to benefit from new developments in information technology. The goals of the reassessment were to: (1) provide an authenticated database containing information and associated metadata for each given HFD value, (2) establish a new evaluation scheme to define HFD quality, and (3) facilitate improvements to the database structure to fulfill the requirements of modern research data infrastructure including database interoperability. In 2021, these efforts resulted in the publication of a substantially renewed GHFD structure (Fuchs et al., 2021a, 2021b), after which the attention focused on how the quality of individual HFD values could be assessed in an objective, comprehensible and well-documented way.

In this paper, we present the new HFD quality evaluation concept. We first introduce the relevant terms for HFD determinations. Second, we outline why HFD data need a robust quality evaluation framework, and third, we propose a new HFD quality evaluation scheme. Finally, we demonstrate the first application of the new quality scheme using real heat-flow data (based on the IHFC data release of 2023 (Global Heat Flow Data Assessment Group et al., 2023), covering 73,033 HFD values) to test the suggested quality evaluation and to discuss benefits and limitations of the methodology. The suggested quality evaluation framework justifies an update of the IHFC database structure as previously defined in Fuchs et al. (2021a) so that the quality evaluation can also be stored alongside each HFD determination within the GHFD.

2. Background on heat flow and heat-flow evaluation

HFD values represent derivative measures and are not direct observations. They depend on the nature, intensity and distribution of subsurface heat sources and sinks, rock thermal properties and the dominant local heat transfer mechanism. Heat is transferred through three different mechanisms: radiation, conduction and convection. Generally, conduction dominates the heat transfer in the lithosphere with two exceptions: (1) convection may dominate where high rock permeability and/or high hydraulic pressure gradients are conducive to significant crustal fluid motion (e.g., plate boundaries, hot spots, geothermal systems or areas with active groundwater flow) (Beardsmore and Cull, 2001); and (2) radiation may become a significant heat transfer mechanism at higher temperatures and pressures in the lower mantle and the core-mantle boundary (Badro et al., 2004).

Heat-flow density is defined as the vertical component of conductive heat transfer in the lithosphere. It is the sum of basal heat flow and internal radiogenic heat production. In principle, HFD (q), is determined using Fourier's law by applying a simple calculation representing the product of the average temperature gradient and the average vertical thermal conductivity over a given depth interval:

$$q = -\lambda_z \frac{dT}{dz}, \quad (1)$$

where dT/dz is the temperature gradient (K/km; z is depth, positive downwards) and λ_z is the vertical thermal conductivity (W/[m·K]). The negative sign in the equation indicates heat flows from hot (high temperature in the Earth) to cold (low temperature at Earth's surface), and thus in the opposite direction to the temperature increase direction.

The temperature gradient is, by definition, a vector quantity dependent on the distribution of temperature in three dimensions. It is assumed that the direction of the maximum gradient within the upper crust is vertical, and therefore the gradient is the derivative of temperature with respect to depth. The gradient dT/dz is evaluated from measurements of temperature from at least two distinct depths. Measurements of subsurface-temperature values for gradient measurements should represent steady-state conditions under the assumption of conductive heat transfer. However, in practice measured temperatures may be affected by near-surface perturbations, such as topographic effects, convective heat transfer (fluid movements), non-steady-state conditions (paleoclimatic effects, sedimentation/erosion, urban heat island effect), and non-vertical (heat refraction) heat transfer components (Haenel et al., 1988; Beardsmore and Cull, 2001).

The average thermal conductivity λ_z used in the heat-flow calculation should represent the characteristic in-situ vertical thermal conductivity of the full interval over which temperature gradient is determined. For sedimentary sequences, the weighted harmonic mean of the conductivities of the constituent lithologies is the preferred averaging method because the temperature change over an interval is proportional to the thermal resistivity (e.g., Powell et al., 1988). Although the determination of in-situ thermal conductivity is possible, it is rarely feasible. To circumvent this problem, thermal conductivity is often determined on extracted core or cutting samples in a laboratory, assumed from nearby lithology, or based on literature values. The effect of temperature, pressure, and fluid saturation on the thermal conductivity also needs to be accounted for together with the geological heterogeneity of the subsurface interval. Thus, a detailed evaluation of HFD data quality requires the designation and consideration of primary data and metadata. Intrinsic quality depends also on the details of the respective HFD determination method. Taking different geological settings and measuring conditions into account, slightly different data types need to be considered. The following section presents the common approaches applied for HFD determination.

2.1. Heat-flow determination

In the past, the IHFC distinguished two different types of heat-flow data: continental and marine. Continental data were those derived from boreholes and mines on the continents and marine data were mainly shallow temperature-probe measurements. Nevertheless, boreholes are drilled in the deep sea as well as probe measurements are made in lakes or rivers on the continents. Therefore, the classical distinction of these two data types as a basis for quality assessment is outdated. The acquisition method is considered a more appropriate attribute for categorizing a HFD determination.

In continental boreholes, temperature gradient should ideally be determined below the deepest level at which temperature is significantly affected by the diffusion of surface climatic temperature perturbations. The most significant temperature gradient deviations were caused by the warming of about 10 to 15 °C, which occurred at the end of the last glaciation period in the Northern hemisphere. The effect of which depends on the locality and can be <1 K/km for the temperature gradient down to a depth of two kilometers (cf. Lotz, 2004; Pauselli et al., 2019).

For marine boreholes and shallow probe measurements, the water column may protect the subsurface temperature field from climatic perturbations. The minimum depth of this "protection effect" in marine settings may vary regionally, possibly depending on oceanographic conditions, but is generally ranging for the water column from 1000 to >4000 m (cf. Haenel, 1979; Ritter et al., 2004; Pascal, 2015). Climate effects on the subsurface temperature distribution are clearly documented in permafrost regions, where the base of permafrost is defined as the depth where the temperature is reaching 0 °C (Osterkamp and Burn, 2003) and which can be as deep as 1493 m, e.g., in the northern Lena and Yana River basins of Siberia, Russia (Desonie, 2008). The effect of post-industrial atmospheric temperature rise is also documented to a depth of ~100 m (cf. Bodri and Cermak, 2007).

Available instruments to measure temperature fall into one of the following classes: (1) wire-line tools and probe-sensing tools being in constant electrical contact with the surface; (2) self-contained thermometers (as used on drill strings for bottom-hole temperature recording); (3) autonomous computer tools with integrated memory units for recording a time-temperature log; (4) distributed optical fiber temperature-sensing systems enabling simultaneous recording over a full borehole interval (e.g., Freifeld et al., 2008). High precision electronic instruments yield the most accurate and precise temperature data capable of resolving temperature gradients at a fine depth resolution.

For an accurate temperature-gradient calculation, it is advantageous to record as many temperature values as possible in a vertical section. However, the process of drilling into the subsurface to measure the temperature will itself disturb the thermal field, requiring thermal re-equilibration times on the order of several minutes for marine probe/borehole measurements and up to several months or years for deeply disturbed continental boreholes. Appropriate corrections need to be considered to obtain equilibrium (undisturbed) temperatures (e.g., Beck and Balling, 1988; Nielsen et al., 1990; Förster, 2001; Schumacher and Moeck, 2020). To allow the thermal disruption to equilibrate, downhole temperature logging should not be attempted until after a period of at least 10–20 times the drilling or fluid circulation (e.g., in fresh water wells) time has elapsed. The temperature gradient is an important input for the HFD quality evaluation, with quality related to the acquisition method and number of temperature data points. In addition, penetration depth, water depth and probe tilt are additional quality criteria that apply to temperature gradients obtained using probe sensing.

In addition to direct techniques, subsurface temperatures may also be estimated using derivative methods, including the Curie point depth (e.g., Tanaka et al., 1999), bottom-simulating reflector (BSR) depth (e.g., Yamano et al., 1982), and lower-crustal high (electrically) conductive layer (e.g., Majorowicz et al., 1993). The Curie point depth is the depth at which rocks in a specific geographical area encounter the Curie temperature and lose their permanent magnetic properties; this is typically around 580 °C, the value for pure magnetite (e.g., Gasparini et al., 1979; Hunt et al., 1995). Based on geophysical studies (including aeromagnetic survey data, spectral analysis, and forward modeling), Curie point depth may be estimated and subsequently used to calculate temperature gradients. The BSR is equivalent to the Curie point depth, where gas hydrate accumulates in the sediment pore water at depth, showing a strong impedance in seismic reflection profiles (White, 1979). The pressure and temperature (p/T) stability field of these hydrates and the seismic profiles can be used to estimate a temperature and depth at the base of the hydrates. Combining these two parameters with a bottom-water temperature and thermal-conductivity values allows an estimation of HFD. In unsedimented volcanic areas offshore, measurements of conductive heat flow can be achieved by covering the surficial rocks using a water-saturated and thermistor-equipped urethane foam acting as a thermal isolation with temperature recordings from below and at the top of the thermal blanket (Johnson and Hutnak, 1997). The mentioned methods have been improving over time, however, they require certain assumptions on the applicability of the method applied in the respective study area which could not be judged in detail. The Curie point depth method representing an approach on a crustal scale will reflect in most cases a rather rough estimate of HFD. A general estimation of the uncertainty of each method is difficult but the uncertainty is usually much higher than those from direct measurements. Further indirect methods for constraining subsurface temperatures make use of different data sources. Some of them have rather poor depth resolution like mineral, hydrochemical, isotopic, fluid, gas or silica geothermometers (e.g., Swanberg and Morgan, 1979) as well as xenolith data (e.g., Boyd, 1973; Kukkonen and Peltonen, 1999) and attenuation of shear waves close to the lithosphere-asthenosphere boundary (i.e. ~1300 °C isotherm, Turcotte and Schubert, 2002). The accuracy of estimated HFD values in case of derivative methods strongly depends on the capability to estimate correctly the rock types in cross-section and their thermal conductivity.

To evaluate HFD quality, information on the methods used to determine temperature gradient is essential (i.e., gradient interval depths, applied method for temperature determination and corrections, if applied).

Rock thermal conductivity is the second major factor to determine the HFD and can be measured in-situ, in the laboratory on recovered core, outcrop or cutting samples or estimated from compilations of values reported in the literature for equivalent lithologies, or measured values from nearby sites. Importantly, because rock and mineral thermal properties are pressure (p) and temperature (T) dependent, thermal-conductivity measurements made on samples in the laboratory may need to be reduced to effective in-situ p-T conditions. Moreover, thermal conductivity can be determined with several different techniques (Appendix A). The most appropriate technique should be selected and applied according to the sample characteristics (origin of the sample, rock type, grain size, texture, sample conditions, expected value range of conductivities, etc.) and their applicability to in-situ conditions. In some methods contact resistance between the sample and experimental apparatus also needs to be considered. Thus, to assess quality, information about the source (e.g., core sample, outcrop, assumed), method, saturation and p-T conditions must be reported together with the thermal-conductivity data.

The assumption of a purely conductive and equilibrated vertical temperature profile which underpins reported values of HFD can be undermined by environmental effects. Temperature gradients and heat flow may be altered by transient effects such as sedimentation, erosion, ground-surface temperature variations (caused by e.g. climatic or land use variations) or variations in bottom water temperatures. Moreover, heat refraction due to lateral thermal-conductivity contrasts may result in HFD values significantly different from the ones that would be measured in an ideal horizontally layered Earth with a smooth top surface. These effects can be important for the HFD quality evaluation.

HFD is mainly determined with two methods: the interval method or the Bullard plot (cf. Powell et al., 1988). The interval method combines the temperature gradient of each depth interval with the representative average thermal conductivity of the associated interval or formation. This method may be affected by data quality and spacing (Beardsmore and Cull, 2001). The Bullard method is based on the concept of thermal resistance (i.e. the reciprocal of the thermal conductivity integrated over depth). HFD is estimated by a linear relationship between the thermal resistance and the equilibrium temperature (if the effect of heat production, for the depth interval in question, is insignificant). Every individual factor that contributes to uncertainty in the thermal-conductivity estimations, or the presence of advective heat transfer, may cause a non-linear relationship between thermal resistance and temperatures in the Bullard method (Bullard, 1939; Sclater and Crowe, 1979). Measurements of subsurface temperatures for the gradient calculations should, as far as possible, represent steady-state conditions under the assumption of conductive heat transfer, or corrections may be needed. Furthermore, if the HFD was determined over an interval at significant depth, the possible addition of heat produced within the overburden may need to be considered for a true representation of heat

loss at the surface. The amount of heat liberated over a unit of time from a unit volume of rock by the decay of unstable radioactive isotopes is defined by the radiogenic heat production. This source term usually increased the HFD with decreasing depth. The rate of heat production below and within the considered interval of HFD determination is assumed to produce a constant effect on measured temperatures over the period of measurement. Natural bodies of high conductive capacity or/and of high heat production (e.g. rock salt or "hot" granitic plutons with relatively high concentrations of radioactive isotopes) may introduce significant non-vertical components to the near-by temperature gradient field when embedded in less conductive or productive rocks. Beside interval method and Bullard plot, other methods are bootstrapping, a statistical hypothesis testing that involves the resampling of a single data set to create a multitude of simulated samples, or heat flow estimation from numerical modeling.

HFD is determined in soft sediments (normally under water; marine onshore or offshore) by estimating undisturbed sediment temperatures using measurements from short sensors attached to drill bits, or customized shallow heat-flow probes with penetration depths from 50 cm to several meters. The word "shallow" refers here to the limited depth of penetration into the soft sediment and not to the water depth. Specialized instruments which penetrate into soft sediment have evolved to investigate steady-state conductive heat flow in the deep ocean. Historically, three types of design are usually categorized. One design was pioneered by Bullard (1954) and involves the use of a thin steel probe with temperature sensors located within the steel probe. A second design developed by Ewing (e.g., Gerard et al., 1962, and references therein) uses a standard core barrel and measures the temperature gradient using sensors (usually thermistors) in fins mounted on the outside of the core barrel. The third type, the violin-bow probe, designed in 1967 and described by Lister (1979), measures temperature using sensors within a 3–5 mm diameter steel tube attached parallel to, but offset from, a strong 10–15 cm diameter steel rod. The thermal conductivity of the soft sediment is usually estimated by the violin-bow probe in-situ by monitoring the temperature rise and decay over time due to a calibrated heat pulse released from a heater within the thin steel tube. Von Herzen upgraded the Ewing outrigger design to measure in-situ thermal conductivity using the continuous heating line source method (Jemsek et al., 1985). More recently, the outrigger design has also been applied to sediment gravity-core tubes equipped with miniaturized autonomous temperature loggers. Thermal conductivity estimates for HFD determinations from Bullard, Ewing and the outrigger autonomous probes usually rely on measurements made on recovered core samples, known relations between sediment properties and thermal conductivity, assumed values from nearby sediment cores, or on lithology/literature data.

In addition to the above methods, several temperature measurements have also been made using short sensor probes attached to the bottom of drill strings during the Deep Sea/Ocean Drilling Programs (e.g., ODP, IODP; Pribnow et al., 2000). For these marine boreholes, the instrumentation was designed to measure the temperature in the undisturbed sediments up to several meters below the bottom of the main hole. The Advanced Piston Corer Temperature Tool (APCT-3, Heesemann et al., 2006), currently used on IODP Expeditions, is attached to the Advanced Piston Corer tool, with strokes of 9.5 m into the sediment during coring operations to obtain equilibrium sediment temperature at the same time a piston core is retrieved. Thermistor probes need a separate wireline run and have limited penetration depth into the sediment (e.g., SET-2, Davis et al., 1997). These tools have advantages as thermal effects from drilling, such as fluid circulation and frictional heating associated with the rotary motion of the drill bit, are almost absent. However, few HFD determinations were made using this method through or around bare rock, and thus, inherently, the determinations did not account for advective heat transfer due to the circulation of water (Louden and Wright, 1989).

HFD determinations in hard rocks or without water coverage generally rely on subsurface temperatures measured by lowering a temperature sensor into a borehole during or after drilling, rather than from temperature probes measuring below the drill bit. In the case of mining/tunneling activities, temperatures for gradient calculations can be recorded at different depths within the mine/tunnel.

2.2. How to evaluate heat-flow data

The evaluation of the global HFD data is aiming to classify the reliability of the acquired data, to provide a profound comparable database and to enable a deeper understanding of the thermal state of the Earth's lithosphere. To judge the reliability and quality of HFD related data, the "correct" characteristics for parameters affecting HFD determinations should be understood.

Temperature information from the subsurface is influenced by all physical properties and processes relevant to the generation and detection of the respective thermal field. From this perspective, every derived HFD value reflects assumptions and interpretations about conditions at the HFD location. For example, the HFD may or may not have been determined over a depth interval under steady-state conditions and perturbed or not perturbed by drilling processes or paleoclimate effects. Therefore, it is mandatory to document, not only the HFD value itself but also the applied techniques for gradient and thermal conductivity determination and assumed or corrected perturbation effects. A "correct" HFD determination requires accurate temperature-depth data (undisturbed temperature gradient), confirmed by information about thermal drilling disturbances and recovery, the hydraulic state of the formation (e.g., information on hydraulic convection or transient signals), and information on the distribution of thermal properties in a direction perpendicular to the Earth's surface.

For the evaluation of the quality of HFD values, knowledge of the following is essential:

1) basic data (name and coordinates of the heat-flow site, depth range of temperature measurements and HFD determination with the respective uncertainties, date of acquisition, etc.),
2) details on the temperature data (kind of measurement, used equipment, instrumental measurement uncertainties),
3) details on the thermal-conductivity data and how the representative thermal conductivity used in HFD determination was determined (applied methods and uncertainties), and.
4) any information on possible perturbing effects on the temperature field (e.g., sedimentation, terrain, heat refraction, paleoclimatic effects).

Information necessary for consistent HFD evaluation is provided in the Appendix.

Researchers were aware of the complexity of accurately determining HFD since the first datum was obtained. Early studies focused on determining new HFD to get a first picture of the Earth's surface heat flow, the general distribution and possible variation of terrestrial surface heat flow. In general, a HFD determination can appear perfectly executed, with depth intervals, temperatures, gradient(s), and thermal conductivities recorded and reported with small mathematical uncertainty (in an optimal case $<1\%$ for temperature gradient and <2 to 5% for thermal conductivity, respectively), resulting in a precise mean HFD value for a specific location (less than $\pm 5\%$). However, uncertainty about whether the value represents a first-order reliable HFD determination may remain. Additional contextual information is required for a proper assessment. For example, the temperature log measured in a specific borehole and used to calculate temperature gradient for a HFD determination could be affected by heat refraction from a nearby salt structure. The authors reporting the HFD value might be aware of this possibility and suggest a correction. Other authors, when determining HFD in a site nearby, might ignore heat refraction and not apply a correction to their data. Furthermore, the thermal conductivity needed

for the HFD determination could be measured four times on the same sample, providing a mean thermal conductivity with a low standard deviation. But the sample may not represent the thermal conductivity over the depth interval of HFD determination. There might also be different HFD determinations at a single location derived and reported over different depths by different researchers. How should one judge which value represents the terrestrial surface heat flow more accurately? There is, therefore, great value in capturing and presenting information about the geological context and steps for data collection, processing and interpretation applied by different authors. To evaluate the quality of HFD data, representing derivative measures of temperature gradients and assumed representative thermal conductivities, the availability and consideration of metadata are mandatory. We do need all relevant metadata at hand and to apply a more holistic evaluation of the provided data.

3. Heat-flow quality evaluation scheme

Several prerequisites are necessary for the introduction of a new quality-evaluation scheme for the GHFD. The most important is that comprehensive relevant metadata for each HFD determination needs to be accessible and stored in the database. For this, a table-based database is no longer applicable. Relational databases allow storing data using a parent-child system, keeping the relevant unique data of a certain HFD site at one level and providing the detailed information for specific depth intervals and their thermal properties on a child level. This principle enables several HFD values to be stored for a site on the child level. A quality evaluation of the HFD values stored in the GHFD should be applied on the child level. Only the HFD value considered to best represent the 'true' undisturbed terrestrial surface heat flow is then linked to the parent level.

The parent-child system for the GHFD was already introduced by Fuchs et al. (2021a). Fig. 1 illustrates the concept and shows the most relevant parameters and processes necessary for HFD data evaluation. The parent level contains unique parameters for a single location (e.g., HFD value and its uncertainty, geographical coordinates, site name as well as other metadata), including the terrestrial surface HFD value deemed the most accurate for the site. Each parent-level entry is associated with at least one child-level entry. The child-level entries contain detailed information about the depth intervals and associated temperature gradients and thermal conductivities of individual HFD determinations, including information about possible environmental perturbations and metadata like primary publication references (Appendix B). In addition, if the same data are used in separate publications each would be recorded as an individual child element. This database structure allows the full documentation of all available data and context for one specific location without losing information, and provides a framework for presenting unambiguous HFD values for each environmental correction applied. The corresponding quality evaluation scheme we present in this paper provides a tool to identify the most accurate HFD value to be linked to the parent level and to provide the most consistent and quality-approved HFD database.

Our proposed scheme for the evaluation of terrestrial surface heat flow data quality relies on three components: an uncertainty quantification (numerical), a methodological rating, and an evaluation of different perturbation effects (Fig. 2). The three components are finally combined into one overall quality score. The advantage of this three-component evaluation is to establish one scheme for all data despite different methodological quality, allowing a quick comparison for a first evaluation. As mentioned above, the quality of each HFD determination is evaluated at the child level of the GHFD, and the site-specific representative terrestrial HFD value is selected or derived from the relevant entries of the child level and elevated to the parent level. The rich metadata associated with each child level entry enables a user to easily search and select HFD values from the GHFD which meet certain quality criteria. In the following, we explain in more detail the three components of the new HFD quality evaluation scheme.

3.1. Uncertainty quantification (U-score)

The first component reflects a numerical quantification of the heat-flow uncertainty and is given by the relative coefficient of variation (COV):

$$COV(\%) = \frac{HFD_{unc}}{HFD_{mean}}, \quad (2)$$

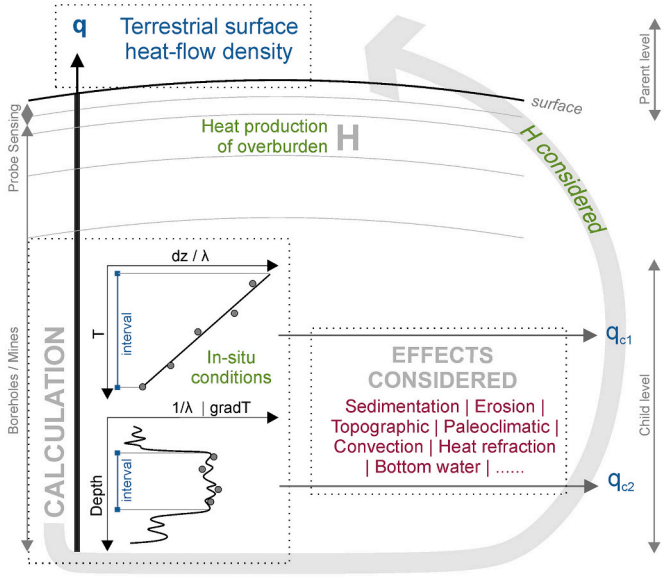

Fig. 1. - Concept of terrestrial surface heat flow q (parent level) and examples of associated heat-flow values qci (child level) after Fuchs et al., 2021a. Abbreviations: H = radiogenic heat production, T = temperature, gradT = temperature gradient, dz./λ = thermal resistance.

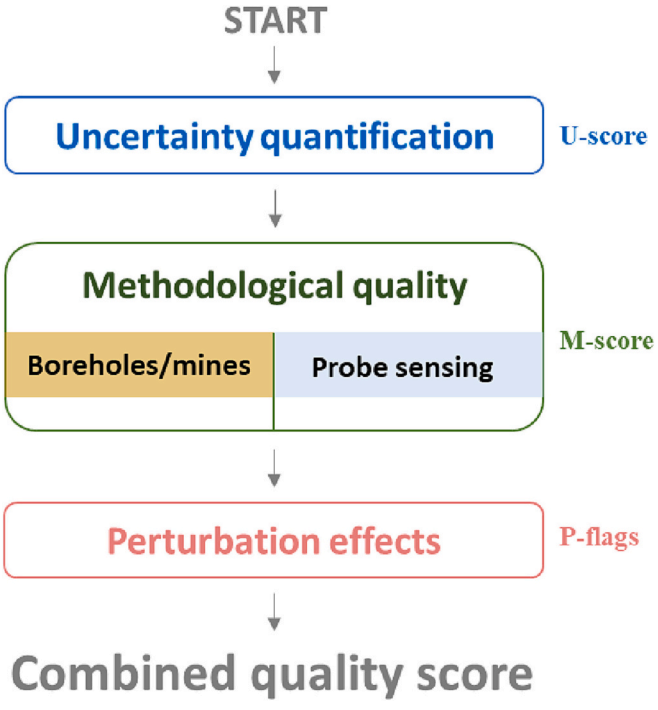

Fig. 2. Workflow of quality evaluation of heat flow data.

Table 1
Definition of the uncertainty classes (U-score) and respective ranking descriptions based on the coefficient of variation.

COV	U-score (Numerical uncertainty)	Ranking description
< 5%	U1	Excellent
5–15%	U2	Good
15–25%	U3	Ok
> 25%	U4	Poor
not applicable	Ux	not determined / missing data

where, HFD_{unc} is the uncertainty of the mean heat-flow density (HFD_{mean}) defined as the arithmetic average HFD value (in mW/m^2). HFD_{unc} is calculated from the error propagation of the uncertainties of the conductivity (λ in W/mK) and temperature gradient ($\frac{\partial T}{\partial z}$ in K/m) implemented in the heat-flow calculation (Taylor, 1997):

$$HFD_{unc} = \sqrt{\left(\lambda_{mean} \cdot \frac{\partial T}{\partial z_{unc}}\right)^2 + \left(\frac{\partial T}{\partial z_{mean}} \cdot \lambda_{unc}\right)^2} \quad (3)$$

For the quantification of the U-score the COV is classified according to Table 1.

3.2. Methodological quality evaluation of thermal conductivity and temperature gradient (M-score)

The second component is based on a score reflecting the inherent accuracy of the methods of temperature gradient and thermal-conductivity determination. This step requires a more complex assessment to reflect the considered background and metadata, accordingly. To honor the methodological differences of shallow probe sensing and the borehole/mine determinations, we differentiated the scoring scheme. For each input parameter (temperature gradient and thermal conductivity), an individual score is determined, which considers – starting with a value of 1.0 – penalties of different values (mostly negative) as ratings for the implemented methods. The penalties are modifying the temperature and conductivity score. In borehole/mine settings, for instance, perturbed bottom-hole temperature measurements have larger penalties than unperturbed temperature logs, whereas in probe-sensing measurements, large penetration depths are afflicted with smaller penalties than small probe penetrations. Based on the final product of the temperature and conductivity score, the overall quality is quantified and used for the classification of the M-score (cf. Fig. 3). The larger the penalties and, thus, the lower the values of the T and TC score, the lower the product and thus the overall quality of the methodological approach. For both types of HFD determinations, the evaluation results in one of four quality classes, ranging from M1 (excellent) to M4 (poor) (Figs. 4 and 5). For datasets with insufficient or missing metadata (empty or unspecified fields), which do not allow to compute all the relevant parameters for T and TC scores, the largest penalty is assumed for the respective parameter. In such cases, an "x" is added to the final M-score to indicate the incomplete data. Then, the M-score will appear like M3x instead of M3.

3.2.1. Evaluation scheme for probe-sensing measurements

3.2.1.1. Temperature gradient. The evaluation criteria considered for the probe-sensing scheme are 1) the probe penetration depth, 2) the number of temperature points used to estimate the temperature gradient, 3) the water depth in mbsl (meters below sea level) and 4) the tilt of the probe. The scoring starts at 1.0 and varies from 0.2 to 1.2. The penetration depth assigns −0.2 for unspecified or shorter penetration depth than one meter, followed by depth ranges of 1–3 (−0.1) and 3–10 m (0), and a bonus of 0.1 for penetration >10 m. The number of temperature points used to estimate the temperature gradient is similar, with four different penalties/bonuses from −0.2 to +0.1 (Table 2). The water depth and probe tilt consist of three penalties from −0.2 to 0, however if both or one of these parameters are corrected for their respective perturbation a score of zero is maintained. All relevant entries are in the form of an integer within the relevant database fields (Table 2).

3.2.1.2. Thermal conductivity. Evaluation criteria for the thermal conductivity quality score include 1) the location, 2) the source type and saturation condition, 3) the number of conductivity measurements and 4) the pressure and temperature conditions. Table 2 shows in detail the score reductions or enhancements based on the defined threshold values. The score starts at 1.0 and varies from 0.2 to 1.2.

The reduction for thermal conductivity data obtained from the literature or unknown location is 0.2, for nearby or other locations 0.1 and for in-situ measurements 0. The source type is divided into three blocks, offshore, onshore and estimated values. Offshore/shipboard measurements are distinguished from in-situ measurements, based on the source database entry and the relevant method, and recovered/saturated conditions selected by the controlled vocabulary in the thermal conductivity saturation database field. The latter selection applies also for onshore laboratory measurements, with the difference that samples are saturated, measured or calculated, by choosing the different relevant methods in the conductivity saturation database field (Table 2). Thermal conductivity estimated from the lithology, literature and water content/porosity or mineral composition are selected by the conductivity method field with penalties of −0.1 and − 0.2, respectively. The number of conductivity points is similar to the points for gradient estimation. Pressure and temperature conditions are controlled by the chosen vocabulary of the relevant methods within the p-T condition database field. The score varies from −0.2 for recorded/unrecorded ambient and unspecified conditions to +0.1 for actual in-situ conditions. Details on the controlled vocabulary and the database fields can be found in the Appendix A.

3.2.2. Evaluation scheme for borehole and mine data

3.2.2.1. Temperature gradient. The temperature gradient scoring, with values ranging from 0.4 to 1.1 and starting at 1.0, includes three evaluation criteria depending on the measurement type, namely, continuous logs, multiple single measurements, and a single together with a surface temperature estimate. This type of separation ensures the consideration of the number of temperature recordings made (Table 3). Each type is then differentiated into equilibrium/corrected or perturbed measurements, the latter having a higher penalty. The continuous log temperature acquisition is considered to have the lowest penalty (0.1 and − 0.1) as recordings contain usually more than three measurement points, followed by multiple single estimates (−0.1 and − 0.5) and one single point measurement (−0.3 and − 0.6). The relevant database entries for the quality evaluation are the top and bottom *temperature method* and in the case of equilibrium or perturbed the *relevant method* used. The relevant methods are limited by a controlled vocabulary and explained in detail in the Appendix A.

3.2.2.2. Thermal conductivity. Thermal-conductivity scoring varies from 0.1 to 1.2. It starts at 1.0 and is modified according to location, source type, number of measurement points, saturation, and p-T conditions (Table 3). Location depends on whether the interval depth is

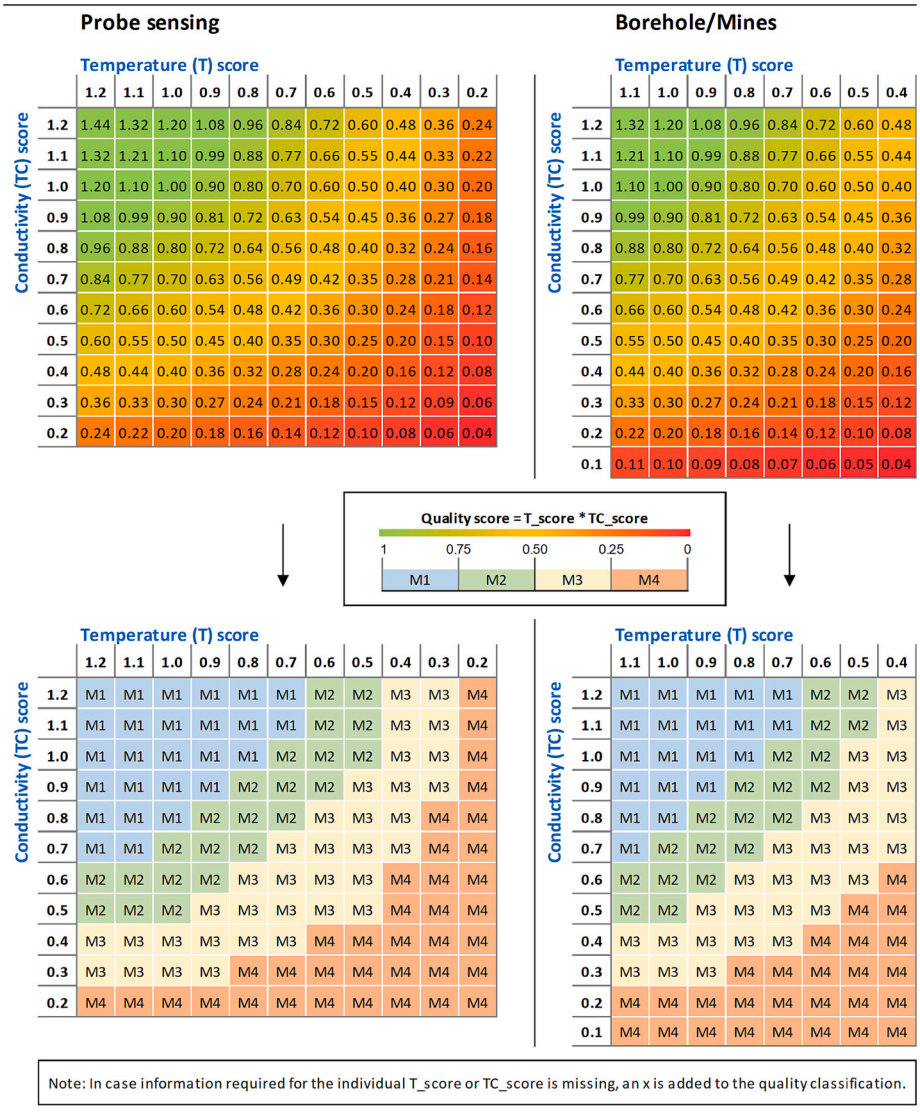

Fig. 3. Definition of the methodological classes (M-score, bottom) and numerical scores (top) for shallow probe sensing (left) and borehole/mine (right) data.

reported or the data originate from a nearby well. In the case that no interval depth is reported, the penalty is −0.9 and the scoring stops, otherwise no penalty is applied. The relevant database fields constraining the decision are top and bottom of the respective heat-flow interval. Three cases of thermal conductivity allocations are considered. The penalty for values from the literature or unknown is −0.2 and from nearby or other locations is −0.1, while if thermal conductivity data are gathered from the actual HFD location no penalty is maintained. The source type penalties vary from 0.1 to −0.2, for in-situ probe measurements/core-log integration and values assumed from general lithology and respective general textbook values, respectively. Scoring is dictated by the thermal conductivity source database field allowing controlled vocabulary entries (Appendix A).

One of two penalties is applied for the number of conductivity points; a neutral rating for >15 measurements and a penalty of −0.1 for 15 or fewer points or if the number of points is unknown. The thermal conductivity number in the database controls this decision.

Saturation and p-T condition penalties are between 0 and − 0.2 and divided by saturated and dry measurements, controlled by the thermal conductivity saturation database entry and both separated for in-situ p-T (p or T individually) and ambient conditions (Table 3). If saturated is chosen, the relevant method within the database field of thermal conductivity p-T conditions controls the penalty, either neutral for in-situ or − 0.1 for ambient conditions. Dry measurements are similar except that penalties for in-situ and ambient p-T conditions are −0.1 and − 0.2, respectively. The combined scoring is presented in Fig. 3, where the temperature is shown on the x-axis and conductivity on the y-axis.

3.3. Recognition of perturbations effects (p-flags)

The third component of the quality assessment concerns possible site-specific perturbation effects. To evaluate the relevance of such effects at a particular site or HFD location and the validity of possible applied site-specific corrections would require much more site-specific information than is actually stored in the database. In principle, the authors of the HFD determination should have discussed perturbations and the applied corrections in their primary publication. In general, the effects of each possible perturbation to the HFD are well understood. But their site-specific relevance and correction approaches are matters of scientific discussion. Nevertheless, perturbation effects could overprint the terrestrial surface heat-flow and for an evaluation of the data it is helpful to know what kind of perturbation effects the respective authors had recognized. Therefore, we propose a pragmatic and helpful indicator: the perturbation flags. These flags consist of seven consecutive letters representing seven different perturbation effects distinguished in the database (details are given in the following). The uppercase letter

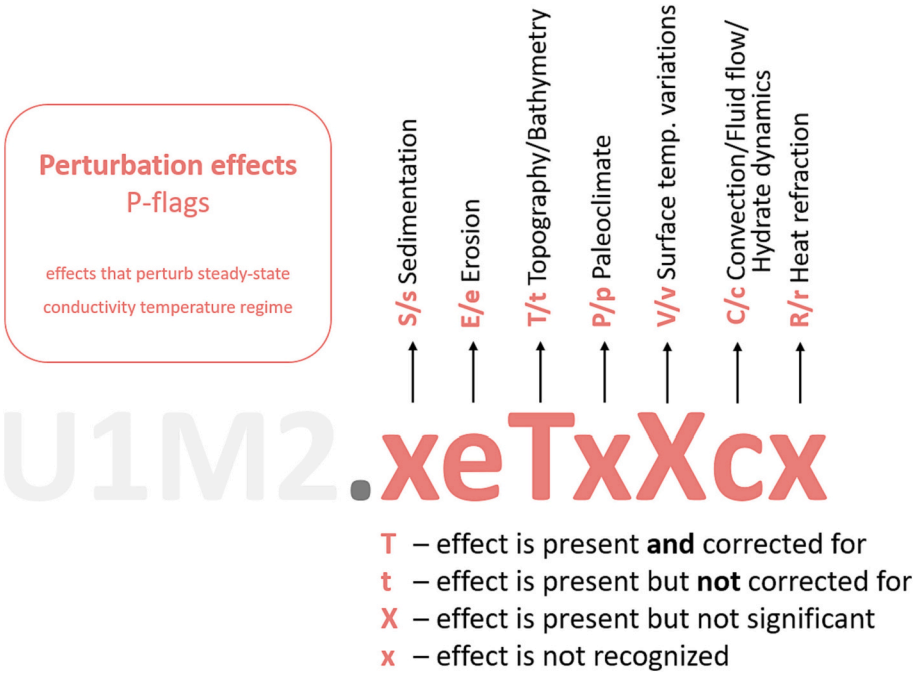

Fig. 4. Example of the coding of perturbation effects (p-flags).

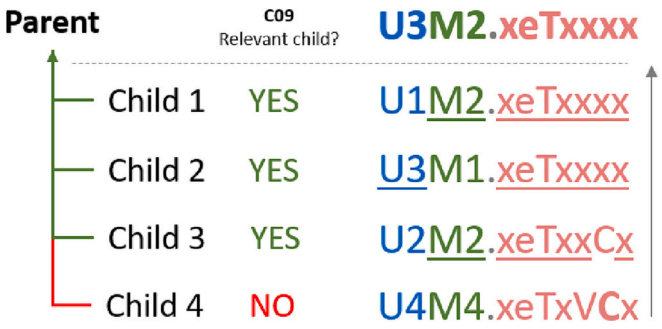

Fig. 5. Example for the inheritance of the combined quality score from child to the parent level.

indicates that the effect is present and corrected, the lowercase letter indicates that the effect is present but not corrected. In the case that the effect is present but assumed to be insignificant an uppercase *X* is used and if the effect is not recognized or assumed to be not present a lowercase *x* is used (see Fig. 4). For data with insufficient information before the assessment took place (empty or unspecified) a minus sign (−) is used at the respective position in the final quality score.

3.3.1. Surface processes / terrain effects: sedimentation (S/s), erosion (E/e), topography/bathymetry (T/t)

Possible thermal effects of a rapid change at the Earth's surface, affecting the temperature field of the subsurface are considered. We distinguish between the effects of sedimentation and erosion. Fast sedimentation changes the former surface temperature condition and decreases the observed HFD, and the cold sediments require some time to return to background conditions. Fast erosion removes large volumes of surface material and exposes deeper strata to the present-day surface conditions. In both cases, the thermal field is not in equilibrium with the present-day boundary condition, whilst for extreme conditions these effects may propagate several kilometers into the subsurface. Significant lateral changes in topography/bathymetry without erosional or sedimentation effects can still cause a change in the surface temperatures that should be included in evaluation of HFD, as well as any necessary correction for 3D terrain effects.

3.3.2. Time-dependent surface temperature effects: paleoclimate/glaciation (P/p), surface/bottom water temperature variations (V/v), convection/fluid flow/hydrate dynamics (C/c)

The diffusion of long-period changes in surface temperature conditions affects the subsurface temperature field within different depth levels. Especially in areas of glaciation and adjacent periglacial regions, disregarding this effect for certain depths will cause flawed terrestrial surface heat-flow determinations. Changes in surface or bottom water temperatures, e.g., in lakes, act in the same direction. A strong influence on the HFD is also possible by advective heat transfer due to active fluid flow by water movement in the borehole or groundwater flow through permeable rocks.

3.3.3. Structural effects: heat refraction (R/r)

Heat refraction affecting HFD can occur due to lateral variations in thermal conductivity. This may be the case at the sediment-basement boundary of sedimentary basins or at salt structures.

3.4. Evaluation of the site-specific HFD quality on the parent level

So far, the evaluation scheme was applied on the child level only. To provide a quality score on the parent level, several cases need to be distinguished. First, if only one child element is present, the score of this entry is simply passed to the parent level. Secondly, if more than one child element is present and all child elements were considered in the calculation of the site-specific HFD value, the poorest ranking is inherited to the parent level (Fig. 5). Thirdly, if more than one child element is present but not all of them were used to calculate a site-specific HFD, only the ones used are considered and the poorest ranking of the relevant child elements is inherited to the parent level again (cf. underlines in Fig. 5).

4. IHFC database structure

As outlined in Section 3, the new quality scheme requires an updated database structure, which is presented below. The updated structure

Table 2
Methodological evaluation scheme (M-score) for shallow probe-sensing data.

Temperature gradient

T score start value: 1.0
value range: 0.2-1.2

Probe penetration

Penetration depth	Relevant DB field(s) full {short}	Relevant methods/entries	Condition in field {...}	Penalty
>10 m	Penetration depth {probe_penetration}	*value*, [Unspecified]	-	0.1
3-10 m				0
1-3 m				-0.1
<1 m OR unspecified				-0.2

Number of temperature points

Number of temperature points	Relevant DB field(s) full {short}	Relevant methods/entries	Condition in field {...}	Penalty
>5	Number of temperature recordings {T_number}	*value*, [Unspecified]	-	0.1
3-5				0
2				-0.1
0-1 OR unspecified				-0.2

Water depth

Depth	Relevant DB field(s) full {short}	Relevant methods/entries	Condition in field {...}	Penalty
>2,500 m OR corrected for BWT	Geographical elevation {elevation}	*value, [Unspecified]*	*{corr_BWT_flag}* = [Present and corrected]	0
>1,500 m			-	-0.1
<1,500 m OR unspecified				-0.2

Tilt

Tilt	Relevant DB field(s) full {short}	Relevant methods/entries	Condition in field {...}	Penalty
0-10° OR corrected	Probe tilt {probe_tilt}	*value, [Unspecified]*	*{corr_IS_flag}* = [Tilt corrected]	0
>10-30°			-	-0.1
>30° OR unspecified				-0.2

Thermal conductivity

TC score start value: 1.0
value range: 0.2-1.2

Localization

Question	Relevant DB field(s) full {short}	Relevant methods/entries	Condition in field {...}	Penalty
TC data from actual heat-flow location?	Thermal conductivity location {tc_location}	[Actual heat-flow location]	-	0
TC data from nearby or other location?		[Other location]		-0.1
TC assumed from literature or unknown localization?		[Literature/unspecified]		-0.2

Source type and saturation

Type	Saturation conditions	Relevant DB field(s) full {short}	Relevant methods/entries	Condition in field {...}	Penalty
Offshore on-board (ship) measurement	in-situ	Thermal conductivity saturation {tc_saturation}	[Saturated measured insitu]	{tc_method} = [Probe - pulse technique] {tc_source} = [*In-situ* probe]	0.1
	recovered / saturated		[Recovered], [Saturated measured]		0
Onshore lab measurement	saturated (meas. / calc.)		[Saturated measured]		0
			[Saturated calculated]		-0.1
	dry		[Dry measured]		-0.2
Estimation	saturated	Thermal conductivity method {tc_method}	[Estimation - from lithology and literature]	{tc_location} = [literature/unspecified]	-0.1
	-		[Estimation - from water content/porosity], [Estimation - from mineral composition]		-0.2

Number of conductivities

Number of conductivity points	Relevant DB field(s) full {short}	Relevant methods/entries	Condition in field {...}	Penalty
>3	Thermal conductivity number {tc_number}	*value*	{tc_location} ≠ [Literature/unspecified]	0
2-3				-0.1
0-1 OR unspecified				-0.2

pT conditions

pT conditions	Relevant DB field(s) full {short}	Relevant methods/entries	Condition in field {...}	Penalty
In-situ pT (or p or T)	Thermal conductivity pT conditions {tc_pT_conditions}	[Actual *in-situ* (pT) conditions]	{tc_method} = [Probe - pulse technique]	0.1
		[Replicated *in-situ* (pT)], [Corrected *in-situ* (pT)]		±0.0
		[Replicated *in-situ* (p)], [Corrected *in-situ* (p)], [Replicated *in-situ* (T)], [Corrected *in-situ* (T)]		-0.1
Ambient pT		[Recorded ambient pT conditions], [Unrecorded ambient pT conditions], [Unspecified]		-0.2

Table 3
Methodological evaluation scheme (M-score) for borehole and mine data.

Temperature gradient

T score start value: 1.0
value range: 0.4-1.1

Source type and number of T points

Measurement type		Relevant DB field(s) full {short}	Relevant methods/entries	Condition in field {...}	Penalty
Continuous T log	equilibrium/ corrected	Temperature method (top) {T_method_top}, Temperature method (bottom) {T_method_bottom}	[LOGeq], [cLOG], [DTSeq], [cDTS]	{T_number} >3	0.1
	perturbed		[LOGpert]		-0.1
Multiple single T point	equilibrium/ corrected		[LOGeq], [cLOG], [DTSeq], [cDTS], [BHT], [DST], [RTDeq], [RTDc], [ODDT-PC], [ODDT-TP]		-0.1
	perturbed		[LOGpert], [DTSpert], [BHT], [DST], [RTDpert], [BLK]		-0.3
	estimated		[CPD], [XEN], [GTM], [BSR]		-0.5
One single T point + surface T	equilibrium/ corrected		[cBHT], [cDST], [RTDeq], [RTDc], [ODDT-PC], [ODDT-TP]	{Temperature_method_top} = [SUR]	-0.3
	perturbed		[BHT], [DST], [RTDpert]		-0.5
	estimated		[CPD], [XEN], [GTM], [BSR]		-0.6

Thermal conductivity

TC score start value: 1.0
value range: 0.1-1.2

Localization

Question		Relevant DB field(s) full {short}	Relevant methods/entries	Condition in field {...}	Penalty
Interval depth reported?	NO	Heat-flow interval top {q_top}, Heat-flow interval bottom {q_bottom}	*value*	-	end: TC score = 0.1
	YES				continue
TC data from actual heat-flow location		Thermal conductivity location {tc_location}	[Actual heat-flow location]	-	0
TC data from nearby or other location			[Other location]		-0.1
TC assumed from literature or unknown localization			[Literature/unspecified]		-0.2

Source type

Measurement type	Relevant DB field(s) full {short}	Relevant methods/entries	Condition in field {...}	Penalty
In-situ probe	Thermal conductivity source {tc_source}	[*In-situ* probe]	-	0.1
Core-log integration		[Core-log integration]		0.1
Core measurements		[Core samples]		0
Cutting measurements		[Cutting samples]		-0.1
Outcrop measurement		[Outcrop samples]		-0.1
Log interpretation		[Well-log interpretation]		-0.1
Mineral calculation (mixing model)		[Mineral computation]		-0.2
Lithology/Textbook		[Assumed from literature]		-0.2

Number of conductivities

Number of conductivity points	Relevant DB field(s) full {short}	Relevant methods/entries	Condition in field {...}	Penalty
>15	Thermal conductivity number {tc_number}	*value*	{tc_location} ≠ [Literature/unspecified]	0
1-15 OR unspecified				-0.1

Saturation

Saturation status	pT conditions	Relevant DB field(s) full {short}	Relevant methods/entries	Condition in field {...}	Penalty
Saturated measured		Thermal conductivity saturation {tc_saturation}	[Saturated measured]	-	0
			[Saturated measured insitu]		
Calculated or recovered			[Saturated calculated]		-0.1
			[Recovered]		
Dry measured			[Dry measured]		-0.2

pT conditions

Saturation	pT conditions	Relevant DB field(s) full {short}	Relevant methods/entries	Condition in field {...}	Penalty
In-situ pT (or p or T)		Thermal conductivity pT conditions {tc_pT_conditions}	[Actual *in-situ* (pT) conditions], [Replicated *in-situ* (pT)], [Corrected *in-situ* (pT)]	-	0
			[Replicated *in-situ* (p)],[Corrected *in-situ* (p)], [Replicated *in-situ* (T)], [Corrected *in-situ* (T)]		-0.1
Ambient pT			[Recorded ambient pT conditions], [Unrecorded ambient pT conditions], [Unspecified]		-0.2

adopted the schemes from Fuchs et al. (2021a), from which the main elements are taken over (parent-child system, new metadata fields, field status system). For details on the change from the structure defined by Jessop et al. (1976) to the version from Fuchs et al. (2021a) we refer to the latter publication. A summary of the new scheme adopted for the quality rating is shown in Table 5, with detailed definitions of the fields and entries including the applicable vocabulary documented in the Appendix A. The Appendix B provides an example of the application of

this new IHFC database structure to an existing dataset.

Besides (a) the introduction of new database fields, mostly motivated due to the requirements of the quality scheme, we combined the borehole/mine and probe-sensing scheme to (b) a unique scheme and introduced (c) a controlled vocabulary for specific entries, as these are crucial for the quality evaluation (for details see Appendix A). Both, the vocabulary, which can be updated with new technology developments, and the combination of the former separated probe and borehole schema enables easier handling for end users. The field ID has been modified by entering a *P* for parent and a *C* for child in front of the field number to distinguish easily between the different levels and to avoid confusion. All data fields relevant to provide information on the HFD data origin and its geographic location are mandatory to ensure a reproducible database. All data fields necessary for applying the new quality scheme are mandatory (Table 5).

4.1. Parent level (P)

On the parent level, 13 data entries are defined: nine of them are shared for probe-sensing and the borehole/mine schemes, and four additional entries are reserved for the borehole/mine scheme. Compared to Fuchs et al. (2021a), two new fields (P10 and P11), both related to the depths of the boreholes/mines, are introduced (Table 4). These additional entries provide further information on the general setting of the reported HFD determination. A former field named "13 heat-flow transfer mechanism" in Fuchs et al. (2021a) was removed from the database. By definition, the reported heat flow should represent conductive conditions. Advective environments are recorded in the respective flag field (e.g., C18 in Table 4). The former fields "16 date of acquisition" and "33 bottom-water temperature" in Fuchs et al. (2021a) were removed from the parent level and introduced in the respective child level (see below).

4.2. Child level (C)

A total of 49 data entries are defined on the child level (Table 4). These entries are grouped into heat-flow (C01–C06), site-specific data (C07–C27), temperature gradient information (C28–C39), and thermal conductivity data (C40–C49).

4.2.1. Heat flow and site-specific metadata

In comparison to Fuchs et al. (2021a), the probe-sensing relevant fields C21 (probe type) and C22 (probe length) were moved from the heat-flow to the site-specific metadata group, resulting in a total of six entries within the heat-flow child group. Because all fields of the heat-flow group are relevant for the overall quality assessment, all are mandatory entries now. In the site-specific metadata group, 20 entries are given. 14 are shared with the borehole/mine and probe-sensing scheme with five additional relevant for probe-sensing. For the latter, a new recommended field (C20) allows information on the Expedition/Platform/Ship whence the primary data were collected. This provides the end-user with a quick overview of additional geophysical and geological data available and is useful for further interpretations. In addition, field C24 (bottom-water temperature) is moved to the child level and set to optional. The main changes in this group relate to the flag fields (C11–C19). An extended vocabulary was provided to these fields to allow a discrimination whether certain effects were corrected or not, but also to distinguish if the effects are present at all or were not recognized by the authors. The fields C25 (lithology) and C26 (stratigraphic age) provide vocabulary according to the IUGS Commission for Geoscience Information (CGI) simple lithology scheme for naming the lithology (http://resource.geosciml.org/classifier/cgi/lithology) and the International Chronostratigraphic Chart of the International Commission on Stratigraphy (https://stratigraphy.org) for naming the stratigraphy, respectively. Details are listed in Appendix A.

4.2.2. Temperature gradient

The measured subsurface temperature and calculated temperature gradients have a first-order control on HFD determination. In this group 12 items are listed, six relevant for both schemes, borehole/mine and the probe-sensing, and an additional six only relevant for the borehole/mine scheme. To reproduce the reported HFD value, the calculated or inferred temperature gradient (C27) needs to be given, although the value itself is not used in the quality evaluation. For the borehole/mine scheme the provision of the depth interval of the respective child entry is mandatory and used in the quality evaluation. The number of temperature recordings (C37) is required for the quality evaluation for both the borehole/mine and the probe sensing scheme. Field C38 (date of acquisition) is a new entry in this group in comparison to Fuchs et al. (2021a). Although this field entry is not used in the evaluation scheme, it is mandatory for a general statistical overview on how many measurements are available for a certain time period, temporal offset of multiple temperature logs at the same borehole, and for the estimation of the effect of bottom water temperature variation.

4.2.3. Thermal conductivity

Eleven fields, relevant for both evaluation schemes, describe the topic of thermal conductivity in the context of HFD determination (Table 4). Most of them are mandatory, only C40 (thermal conductivity uncertainty), C46 (thermal conductivity p-T assumed function), and C48 (thermal conductivity averaging) are recommended and the provision of an international generic sample number (IGSN, C49) is optional. For evaluation, the thermal conductivity method (C43) is only mandatory for the probe-sensing evaluation scheme. For borehole data, the variety of methods with different reliability depending on the source material precludes an automatic, unambiguous consideration of the conductivity method in the evaluation scheme. Compared to Fuchs et al. (2021a), a new data entry, C42 (thermal conductivity location) is introduced to specify whether the thermal conductivity was determined at the same location of the HFD or based on alternative sources.

4.3. Database administration level (A)

The fields in this group are used for database queries and administration purposes only. These entries are visible but not editable by a general user and are related to the corresponding child/parent level and contain information on the HFD site itself (A4–A8) and on the metadata of data (re-)assessment (fields A1–A3). Invisible administration fields are used for data linkage and organization.

5. Discussion

The reorganization and modification of the GHFD provides a transparent and authenticated database, enabling a comprehensible evaluation of the accessible heat-flow data from different user perspectives. Every heat-flow determination represents certain thermal conditions and methodological assumptions. Based on consistent and thorough documentation of the heat-flow determination our scheme allows an evaluation of the quality of heat-flow data according to three main criteria. In contrast to former approaches to data quality classification, which assigned one single subjective quality code to each heat-flow value (e.g., "excellent" or "moderate"), the new approach allows an

Table 4
Adopted new database structure showing associated data fields for the parent and child level [Level] relevant for HFD determinations [Domains] from borehole and mines (B) and for shallow probe-sensing data (S). Database fields [Obligation] are classified as mandatory (M), recommended (R), or optional (O). The relevance for the quality evaluation [Quality] is displayed for the U-score (U), the M-score (M) and the perturbation effects (P).

ID	Field name		Domain	Obligation	Quality	Level
P01	Heat-flow value		B,S	M	U-score (B,S)	Parent
P02	Heat-flow uncertainty		B,S	M	U-score (B,S)	
P03	Site name		B,S	M		
P04	Latitude (Geographical)		B,S	M		
P05	Longitude (Geographical)		B,S	M		
P06	Elevation (Geographical)		B,S	M	M-score (S)	
P07	Basic geographical environment		B,S	M		
P08	General comments parent level		B,S	R		
P09	Flag heat production of the overburden		B,S	R		
P10	Total measured depth		B	R		
P11	Total true vertical depth		B	R		
P12	Type of exploration method		B	M		
P13	Original exploration purpose		B	R		
C01	Heat-flow value child	Heat flow	B,S	M	U-score (B,S)	Child
C02	Heat-flow uncertainty child		B,S	M	U-score (B,S)	
C03	Heat-flow method		B,S	M		
C04	Heat-flow interval top		B,S	M	M-score (B, S)	
C05	Heat-flow interval bottom		B	M	M-score (B)	
C06	Penetration depth		S	M	M-score (S)	
C07	Primary publication reference	Meta data	B,S	M		
C08	Primary data reference		B,S	R		
C09	Relevant child		B,S	M		
C10	General comments child level		B,S	R		
C11	Flag in-situ thermal properties		B,S	R		
C12	Flag temperature corrections		B,S	M	M-score (S)	
C13	Flag sedimentation effect		B,S	M	P-flag	
C14	Flag erosion effect		B,S	M	P-flag	
C15	Flag topographic effect		B,S	M	P-flag	
C16	Flag paleoclimatic effect		B,S	M	P-flag	
C17	Flag surface temperature/bottom water		B,S	M	P-flag	
C18	Flag convection processes		B,S	M	P-flag	
C19	Flag heat refraction effect		B,S	M	P-flag	
C20	Expeditions/Platforms/Ship		B,S	R		
C21	Probe type		S	R		
C22	Probe length		S	R		
C23	Probe tilt		S	M	M-score (S)	
C24	Bottom-water temperature		S	O		
C25	Lithology		B,S	O		
C26	Stratigraphic age		B,S	O		
C27	Calculated or inferred temperature gradient	Temperature gradient	B,S	M		
C28	Temperature gradient uncertainty		B,S	R		
C29	Mean temperature gradient corrected		B,S	O		
C30	Corrected temperature gradient uncertainty		B,S	O		
C31	Temperature method (top)		B	M	M-score (B)	
C32	Temperature method (bottom)		B	M	M-score (B)	
C33	Shut-in time (top)		B	R		
C34	Shut-in time (bottom)		B	R		
C35	Temperature correction method (top)		B	R		
C36	Temperature correction method (bottom)		B	R		
C37	Number of temperature recordings		B,S	M	M-score (B, S)	
C38	Date of acquisition		B,S	M		
C39	Mean thermal conductivity	Thermal conductivity	B,S	M		
C40	Thermal conductivity uncertainty		B,S	R		
C41	Thermal conductivity source		B,S	M	M-score (B, S)	
C42	Thermal conductivity location		B,S	M	M-score (B, S)	
C43	Thermal conductivity method		B,S	M	M-score (S)	
C44	Thermal conductivity saturation		B,S	M	M-score (B, S)	
C45	Thermal conductivity pT conditions		B,S	M	M-score (B, S)	
C46	Thermal conductivity pT assumed function		B,S	R		
C47	Thermal conductivity number		B,S	M	M-score (B, S)	
C48	Thermal conductivity averaging methodology		B,S	R		
C49	IGSN		B,S	O		
A1	Reviewer name		x			Admin
A2	Reviewer comment		x			
A3	Review date		x			
A4	Country		x			
A5	Region		x			
A6	Continent		x			
A7	Domain		x			
A8	Unique entry ID		x			

automated, data-driven classification and a transparent assessment of possible perturbing effects. In the following section we discuss the new scoring system, its upcoming application to the re-organized GHFD, and the expected benefits and limitations of the new approach in more detail.

5.1. The new scoring system

Some examples for quality ranking of heat-flow determinations were provided in Richards et al. (2012). Most approaches try to provide simple quality containers, considering the mean error within gradient measurements (Jessop et al., 1976), the variation of heat-flow over a small area (Balling et al., 1981), or depending on the interval length (Blackwell et al., 1991). Richards et al. (2012) proposed a parameter-weighted evaluation system discriminating between "conventional" and "bottom-hole temperature" heat-flow sites. Depending on the respective evaluation scheme, reliability values are assigned for certain parameters (e.g., for temperature and thermal conductivity data and heat-flow correction procedures) that then could be analyzed further or combined to an overall score. According to Richards et al. (2012), their "reliability code" should offer "the user a visual list of items to review and questions to ask about the data". This idea is developed further in our new evaluation approach. We established the tripartite quality code to improve the visualization of quality-relevant (meta)data, allowing a discrimination between quality rating due to numerical uncertainty (U-score), the methodological approach (M-score), and of environmental, site-specific effects (P-flags). The code can also be used as a selection criteria, so that heat-flow data conforming to particular quality requirements could be selected according to specific research interests of the respective user. In contrast to Richards et al. (2012), we apply one of two different evaluation schemes depending on the type of heat-flow determination regime, i.e. for shallow probe-sensing or for data from boreholes/mines. Table 5 shows examples of quality assessments for generic data. Several observations can be made: 1) the uncertainty code provides information on the mathematical uncertainty only. Heat-flow represents a physical quantity based on measured properties which need to be reported in the database, so the uncertainty score is a parameter that could be provided easily by applying simple mathematics. The natural geological heterogeneities involved in heat-flow determination may easily outweigh the uncertainty based on error propagation, but the U-score allows us to assess the mathematical variance independent from those effects. A good U-score (U1) alone, however, is not a guarantee for a high-standard total heat-flow determination. 2) The M-score evaluates the respective methods applied for gradient and thermal conductivity determination. The scoring starts from a base value of 1 for each parameter. This equal weighting is justified by the Fourier equation for heat-flow determination and is also considered in the approach of Richards et al. (2012). While Richards et al. (2012) consider the used temperature gradient and the underlying temperature measurement separately, we evaluate the temperature gradient in one step (source type). In our new scheme, however, missing metadata ('=M=' in Table 5) results in a conservative maximum penalty for this entry. This shall also motivate authors to provide all necessary metadata to the GHFD. The application of the scoring to probe-sensing gradient data is more differentiated than borehole/mines gradient data. However, the reader should keep in mind that also in the latter eight cases are considered under the term "source type and number of temperature points". 3) The P-flag requires comprehensive, site-specific heat-flow metadata. Most entries in the database are not yet filled with this information.

5.2. Application to data release 2023

Implementation of the new quality scheme (section 3) requires modifications to the previous database structure and field definitions, demanding also a reassessment of the stored data. With the new quality scheme presented here, additional data or the use of an adopted vocabulary for already existing database fields is necessary. This will be considered in the on-going and future assessment process, including also a further re-assessment of the already revised share of data in the light of the new requirements. About 20% of data (ca. 13,000 data points) of the current data release (Global Heat Flow Data Assessment Group et al., 2023) were revised in terms of the structure and definition defined in Fuchs et al., 2021a. The quality scheme can be applied without the new fields and definitions, but without this information the majority of quality assessments would be loaded with extra penalties for missing data yielding an artificial bias of the methodological rating (M-score) towards the lower ratings. For most of the sub groups of the conductivity or temperature-gradient evaluation, this penalty for missing data amounts to −0.2. Considering the interplay between the ranges of the individual conductivity and temperature-gradient scores and the total classification scheme for the M-score (thresholds at 0.75, 0.5 and 0.25), such a penalty quickly results in a downgrading by one class. This highlights the value of careful documentation of heat-flow metadata to avoid an unnecessary downgrading.

From a small, already complete subset of data ($n = 143$; borehole/mine data only, ca. 1% of reassessed data), we can derive impressions on the methodological ratings (Fig. 6). Here, only a quarter of data achieves the better M1 and M2 ratings, while nearly half of the entries are rated as M4. More in-depth analysis of the quality distribution and statements on its impact have to wait until the new structure is adopted and considered during the assessment of larger parts of the database (Global Heat Flow Data Assessment project; http://www.ihfc-iugg.org). Specific data examples for the application of the scheme are documented in the Appendix B.

5.3. Expected benefits and limitations of the IHFC quality evaluation approach

In contrast to former approaches to quality evaluation, the scheme allows us to assess the quality of data from different heat-flow determination settings (borehole/mine and probing) at a glance. The combined score considers different dimensions of quality: numerical uncertainty aspects, the methodological quality of temperature and thermal conductivity determinations needed for heat-flow determination, and the possibility of (overriding) perturbing site-specific effects. This evaluation represents the first comprehensive deterministic approach to describe the quality of heat-flow data based on a well-documented, comprehensible, and consistent procedure. For the evaluation, the provision of a well maintained database comprising all necessary metadata is mandatory. To provide unambiguous field entries, a set of pre-defined vocabulary for relevant fields was determined that will also facilitate the collection of new heat-flow data and that can be adapted or extended on demand. Because the current approach is based on an algorithmic scoring system and can be calculated programmatically, quality values can also be recalculated easily if the scheme should evolve without complete re-evaluation of the database. However, the application of the scheme requires an extended set of database fields compared to the former GHFD compilations.

Table 5
Application of the scoring system to the examples reported in Appendix B. For the M-score, the penalties for the elements of T score and TC score are listed. Therein, missing entries are shown as = M = and considered with the maximum penalty of the respective element (cf. Tables 2 and 3).

Score		Example:	A	B	C	D	E	F	G	H	I	J
			Probe sensing (S)					Borehole/Mine (B)				
			Location 1			Location 2		Well 1	Well 2	Well 3		
U		COV	3.7%			2.7%		4.5%	2.0%	16.4%		
		U score	**U1**			**U3**		**U1**	**U1**	**U3**		
M	Temp	Penetration	-0.10	0.00	-0.10	0.10	0.00	Source -0.10	-0.10	0.10	-0.50	-0.30
		Number	0.1	0	0.1	0	0					
		Water depth	-0.2	-0.2	-0.2	-0.2	-0.2					
		Tilt	0	0	-0.1	0	-0.1					
		T score	**0.80**	**0.80**	**0.70**	**0.90**	**0.70**	**0.90**	**0.90**	**1.10**	**0.50**	**0.70**
	Cond	Localization	0.00	0.00	-0.10	0.00	0.00	0.00	0.00	0.00	0.00	0.00
		Source	0.00	0.00	0.00	0.00	0.00	0.10	0.00	-0.10	0.00	-0.20
		Number	0.00	0.00	0.00	0.00	0.00	-0.10	-0.10	-0.10	-0.10	-0.10
		PT conditions	0.00	=M=	=M=	0.00	0.00	0.00	-0.10	0.00	-0.20	0.00
								0.00	=M=	-0.10	=M=	=M=
		TC score	**1.00**	**0.80**	**0.70**	**1.00**	**1.00**	**1.00**	**0.60**	**0.70**	**0.50**	**0.50**
		M-score value	**0.80**	**0.64**	**0.49**	**0.90**	**0.70**	**0.90**	**0.54**	**0.77**	**0.25**	**0.35**
		M score	**M1**	**M2x**	**M3x**	**M1**	**M2**	**M1**	**M2x**	**M1**	**M4x**	**M3x**
P		Sedimentation	S	S	S	S	S	-	S	-	S	-
		Erosion	x	x	x	x	x	-	x	-	r	-
		Topo/Baryth	x	x	x	x	x	-	x	-	T	-
		Palaeoclimate	x	x	x	x	x	-	-	-	P	-
		Surf. Temp. Variation	C	C	C	C	C	-	-	-	-	-
		Convection	x	x	x	V	x	-	-	-	-	-
		Heat refraction	h	h	h	h	h	-	H	-	H	-
			SxxxCxh	**SxxxCxh**	**SxxxCxh**	**SxxxCVh**	**SxxxCxh**	**-------**	**Sxx---H**	**-------**	**SrTP--H**	**-------**
		Combined score	U1M1.SxxxCxh	U1M2x.SxxxCxh	U1M3x.SxxxCxh	U1M1.SxxxCVh	U1M2.SxxxCxh	U1M1.-------	U1M2x.Sxx---H	U2M1.-------	U2M4x.SrTP--H	U3M3x.-------

	Location 1	Location 2
Inherited parent score	U1M3x.SxxxCxh	U1M2.SxxxCxh

Well 1	Well 2	Well 3
U1M1.-------	U1M2x.Sxx---H	U3M3x.-------

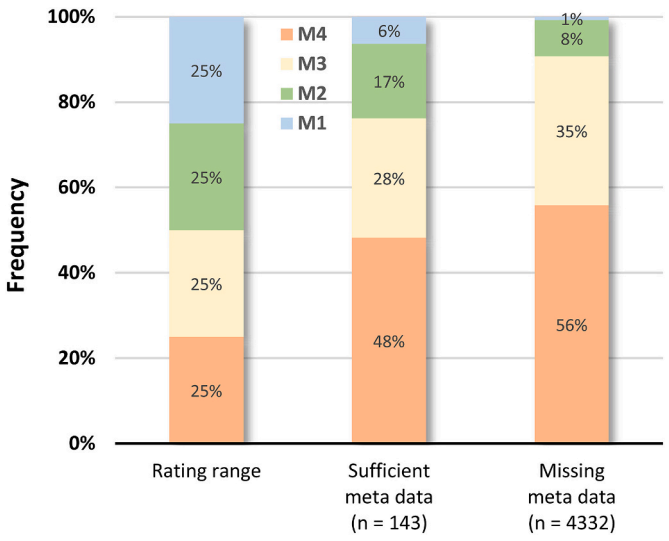

Fig. 6. Example for the statistical distribution of the M-score, differentiated for sufficiently documented entries (according to the demands of the quality scheme) and for data with missing metadata. Data considered are from the revised share of data from Global Heat Flow Data Assessment Group et al. (2023).

6. Summary and Outlook

The new quality scheme, for the first time, allows combining all three relevant dimensions of heat-flow-data quality (quantified uncertainty, methodological quality, status of overruling effect) in one combined score. It allows a quick comparison of heat flow data and reveals missing data or insufficient documentation at one glance. With the new quality scheme, users can select appropriate heat-flow values according to their specific research needs. The adopted and extended database structure makes it possible to interconnect the GHFD to other digital data resources like map data (continents, geology, ocean region), sample data (IGSNs), library services (DOI), etc. In the future, new data relevant to heat-flow determinations may be generated through the interpretation of spatial exploration data and satellite images (e.g. spatial data of bottom surface reflections or other temperature raster data). Such data may be linked to the GHFD as an add-on service in a separate database. A restructured version of the existing database, which will contain the first systematic application of the quality scheme presented here will be published in early 2024. The process of data screening and revision of incomplete, wrong or empty data entries will be an ongoing process for more years to come. The suggested penalty scheme used for the evaluation represents the current consensus opinion of a broad cross section of the scientific community. However, the authors acknowledge and encourage ongoing discussion and adaptation of the scheme as experience of its application is gained.

Funding

This work was supported by the German Research Foundation DFG [grant number 491795283].

CRediT authorship contribution statement

Sven Fuchs: Conceptualization, Methodology, Writing – original draft, Writing – review & editing, Visualization. **Ben Norden:** Conceptualization, Methodology, Writing – original draft, Writing – review & editing. **Florian Neumann:** Methodology, Conceptualization, Writing – original draft, Writing – review & editing. **Norbert Kaul:** Methodology, Writing – original draft. **Akiko Tanaka:** Methodology, Writing – original draft. **Ilmo T. Kukkonen:** Methodology, Writing – original draft. **Christophe Pascal:** Methodology, Writing – original draft. **Rodolfo Christiansen:** Methodology, Writing – original draft. **Gianluca Gola:** Methodology, Writing – original draft. **Jan Šafanda:** Methodology. **Orlando Miguel Espinoza-Ojeda:** Methodology, Writing – original draft. **Ignacio Marzan:** Writing – original draft, Writing – review & editing. **Ladislaus Rybach:** Methodology, Writing – original draft. **Elif Balkan-Pazvantoğlu:** Writing – original draft, Writing – review & editing. **Elsa Cristina Ramalho:** Methodology, Writing – original draft. **Petr Dědeček:** Methodology, Writing – original draft. **Raquel Negrete-Aranda:** Methodology, Writing – original draft. **Niels Balling:** Methodology, Writing – original draft. **Jeffrey Poort:** Methodology, Writing – original draft, Writing – review & editing. **Yibo Wang:** Methodology, Writing – original draft. **Argo Jõeleht:** Methodology, Writing – original draft, Writing – review & editing. **Dušan Rajver:** Methodology, Writing – original draft. **Xiang Gao:** Methodology, Writing – original draft. **Shaowen Liu:** Methodology, Writing – original draft. **Robert Harris:** Methodology, Writing – original draft, Writing – review & editing. **Maria Richards:** Methodology, Writing – original draft, Writing – review & editing. **Sandra McLaren:** Methodology, Writing – original draft. **Paolo Chiozzi:** Methodology, Writing – original draft. **Jeffrey Nunn:** Methodology, Writing – review & editing. **Mazlan Madon:** Methodology, Writing – original draft. **Graeme Beardsmore:** Methodology, Writing – original draft. **Rob Funnell:** Methodology, Writing – original draft. **Helmut Duerrast:** Methodology, Writing – original draft. **Samuel Jennings:** Methodology, Writing – original draft. **Kirsten Elger:** Methodology, Writing – original draft. **Cristina Pauselli:** Methodology, Writing – original draft. **Massimo Verdoya:** Methodology, Writing – original draft.

Declaration of Competing Interest

The authors declare that they have no known competing financial interests or personal relationships that could have appeared to influence the work reported in this paper.

Data availability

No data was used for the research described in the article.

Acknowledgments

The International Heat Flow Commission (IHFC) initiated the discussion on the revision of the Global Heat Flow Database during the 27th International Union of Geodesy and Geophysics (IUGG) General Assembly (Montreal, Canada, 07/2019). Right on time for the 60th anniversary of the IHFC at the upcoming 28th IUGG General Assembly (Berlin, Germany, 07/2023), the new quality scheme and the adopted new structure presented here is a major public result of this initiative. Numerous scientists, many current and former members of the IHFC, have contributed to the discussion, opening new perspectives and sharing their experiences. We would like to thank namely (in alphabetic order): Irina Artemieva, Vladimír Čermák, Christoph Clauser, Andrea Förster, Valiya Mannathal Hamza, Derrick Hasterok, Shaopeng Huang, Alan Jessop, Francis Lucazeau, Sukanta Roy, and Jan Szewczyk. Finally, we thank Carol Stein, and one anonymous reviewer for their review and suggestions for improvements.

Appendix A. Structure and field definitions of the IHFC Global Heat Flow Database

ID	Field name	Short name	Unit	Field type	Obligation	Level	Domain	Group	Quality relevance	Field Description	Allowed range of values	Value description	Choice Box
P01	**Heat-flow value**	q	mW/m²	Float (1 decimal place)	M	P	B,S	Meta	U score	Heat-flow density (q) for the location after all corrections for instrumental and environmental effects.	-999,999.9 – 999,999.9	-	no
P02	**Heat-flow uncertainty**	q_uncertainty	mW/m²	Float (1 decimal place)	M	P	B,S	Meta	U score	Uncertainty (one standard deviation) of the heat-flow value [q] estimated by an error propagation from uncertainty in thermal conductivity and temperature gradient, standard deviation from the average of the heat flow intervals or deviation from the linear regression of the Bullard plot	0 – 999,999.9	-	no
P03	**Site name**	name	-	Char (255)	M	P	B,S	Meta	-	Specification of the (local) name of the related heat-flow site or the related survey. Should be consistent with the publication.	-	-	no
P04	**Latitude (Geographical)**	lat_NS	degrees	Float (5 decimal places)	M	P	B,S	Meta	-	Latitude (lat) is a geographic coordinate that specifies the North–South (NS) position of a point on the planetary surface. The Equator has a latitude of 0°, the North Pole has a latitude of 90° North (written +90), and the South Pole has a latitude of 90° South (written –90). Numeric values (2 digits) with 5 decimal places are used for this database item instead of the N or S format (e.g., -80.00000 instead of 80° S).	-90.00000 – +90.00000	Coordinate according to ISO 6709. The datum is WGS84.	no
P05	**Longitude (Geographical)**	long_EW	degrees	Float (5 decimal places)	M	P	B,S	Meta	-	Longitude (long) is a geographic coordinate that specifies the east–west (EW) position of a point on the planetary surface. The Prime Meridian, which passes near the Royal Observatory, Greenwich, England, is defined as 0° longitude by convention. Positive longitudes are east of the Prime Meridian, and negative ones are west. Numeric values (3 digits) with 5 decimal places are used for this database instead of the E or W format (e.g., -50.00000 instead of 50° W).	-180.00000 – +180.00000	Coordinate according to ISO 6709. The datum is WGS84.	no
P06	**Elevation (Geographical)**	elevation	m	float (1 decimal places)	M	P	B,S	Meta	M score (probe sensing)	The elevation of a geographic location is its height above (land elevation) or below (water depth) mean sea level. *Caution: different national reference systems are used. Also the reference level may be diverse depending on the study (drilling, lake, marine…).*	-12000 – +9000	-	no
P07	**Basic geographical environment**	environment	-	Char (255)	M	P	B,S	Meta	-	Describes the general geographical setting of the heat-flow site (not the applied methodology).	[Onshore (continental)] [Onshore (lake, river, etc.)] [Offshore (continental)] [Offshore (marine)] [unspecified]	-	yes
P08	**General comments parent level**	p_comment	-	Char (255)	R	P	B,S	Meta	-	Comments on the reported heat-flow location value.	-	-	no
P09	**Flag heat production of the overburden (heat-flow correction)**	corr_HP_flag	-	BIT field	R	P	B,S	Meta	-	Specifies if corrections to the calculated heat flow considers the contribution of the heat production of the overburden to the terrestrial surface heat flow q.	[Yes] [No] [unspecified]	-	yes
P10	**Total measured depth**	total_depth_MD	m	float (1 decimal places)	R	P	B	Meta	-	Specification of the total measured depth below mean sea level. *Caution: different national reference systems are used. Also the reference level may be diverse depending on the study (drilling, lake, marine…).*	-12,000 – +9,000	-	no
P11	**Total true vertical depth**	total_depth_TVD	-	float (1 decimal places)	R	P	B	Meta	-	Specification of the total true vertical depth below mean sea level. *Caution: different national reference systems are used. Also the reference level may be diverse depending on the study (drilling, lake, marine…).*	-12,000 – +9,000	-	no
P12	**Type of exploration method**	explo_method	-	Char (255)	M	P	B	Meta	-	Specification of the general means by which the rock was accessed by temperature sensors for the respective data entry.	[Drilling] [Mining] [Tunneling] [Probing (onshore/lake, river, etc.)] [Probing (offshore/ocean)] [Other (specify in comments)] [unspecified]	-	yes
P13	**Original exploration purpose**	explo_purpose	-	Char (255)	R	P	B	Meta	-	Main purpose of the reconnaissance target providing access for the temperature sensors.	[Hydrocarbon] [Underground storage] [Geothermal] [Groundwater] [Mapping] [Mining] [Research] [Tunneling] [Other (specify in comments)] [unspecified]	-	yes
C01	**Heat-flow value child**	qc	mW/m²	Float (1 decimal place)	M	C	B,S	Heat flow	U score	Any kind of heat-flow value (qc).	-999,999.9 – 999,999.9	-	no
C02	**Heat-flow uncertainty child**	qc_uncertainty	mW/m²	Float (1 decimal place)	M	C	B,S	Heat flow	U score	Uncertainty (one standard deviation) of the heat-flow value [qc] estimated by an error propagation from uncertainty in thermal conductivity and temperature gradient or deviation from the linear regression of the Bullard plot (corrected preferred over measured gradient).	0 – 999,999.9	-	no

Meta - Meta data, Heat flow - Heat flow data, Temp - Temperature data, Cond - Thermal conductivity data, Admin - Adminstration data

ID	Field name	Short name	Unit	Field type	Obligation	Level	Domain	Group	Quality relevance	Field Description	Allowed range of values	Value description	Choice Box
C03	**Heat-flow method**	q_method	-	Char (255)	M	C	B,S	Heat flow	-	Principal method of heat-flow calculation from temperature and thermal conductivity data. *Allowed entries: controlled vocabulary*	[Interval method] [Bullard plot] [Boot-strapping] [Numerical inversion] [Other (specify in coments)]	[Interval method]: Fourier's Law or Product or Interval method - product of the mean thermal gradient to the mean thermal conductivity with reference to a specified depth interval]; [Bullard plot]: heat-flow value given as the angular coefficient of the linear regression of the thermal resistance vs. temperature data (used when there is a significant variation of thermal conductivity within the depth range over which the temperatures have been measured)]; [Boot-strapping]: iterative procedure aimed at minimize the difference between the measured and modelled temperatures by solving the 1-D steady-state conductive geotherm (radiogenic heat production of rocks is accounted for); [Numerical inversion]: Computational inversion of borehole heat transport model	yes
C04	**Heat-flow interval top**	q_top	m	Float (2 decimal places)	M	C	B,S	Heat flow	M score	Describes the true vertical depth (TVD) of the top end of the heat-flow determination interval relative to the land surface/seafloor.	0 – 19,999.99	-	no
C05	**Heat-flow interval bottom**	q_bottom	m	Float (2 decimal places)	M	C	B	Heat flow	M score	Describes the true vertical depth (TVD) of the bottom end of the heat-flow determination interval relative to the land surface.	0 – 19,999.99	-	no
C06	**Penetration depth**	probe_penetration	m	Float (2 decimal places)	M	C	S	Heat flow	M score	Penetration depth of marine probe into the sediment.	0 – 999.99	-	no
C07	**Primary publication reference**	publication_reference	-	Char (255)	M	C	B,S	Meta	-	References of primary publication related to the respective heat-flow entry.	[First author_Year_Title_Journal/ Publisher_doi]	-	no
C08	**Primary data reference**	data_reference	-	Char (255)	R	C	B,S	Meta	-	References of primary data publication related to the respective heat-flow entry.	[First author_Year_Title_Journal/ Publisher_doi]	-	no
C09	**Relevant child**	relevant_child	-	Boolean field	M	C	B,S	Meta	-	Specifies whether the child entry is used for computation of representative location heat-flow values at the parent level or not.	[Yes] [No] [unspecified]	-	yes
C10	**General comments child level**	c_comment	-	Char (255)	R	P	B,S	Meta	-	Comments and further specifications to the individual reported heat-flow determination.	-	-	no
C11	**Flag in-situ thermal properties**	corr_IS_flag	-	Char (255)	M	C	B,S	Meta	M score	Specifies whether the in-situ pressure and temperature conditions were considered to the reported thermal conductivity value or not.	[Considered – p] [Considered – T] [Considered – pT] [not Considered] [unspecified]	-	yes
C12	**Flag temperature corrections (instrumental correction)**	corr_T_flag	-	Char (255)	M	C	B,S	Meta	-	Specifies if instrumental corrections to the measured temperature data were required and performed, e.g. for the tilt correction of probes.	[Tilt corrected] [Drift corrected] [not corrected] [Corrected (specify)] [unspecified]	-	yes
C13	**Flag sedimentation effect (temperature/heat flow correction)**	corr_S_flag	-	Char (255)	M	C	B,S	Meta	P score	Specifies if sedimentation/subsidence effects with respect to the reported heat-flow value were present and if corrections were performed.	[Present and corrected] [Present and not corrected] [Present not significant] [not recognized] [unspecified]	-	yes
C14	**Flag erosion effect (heat-flow correction)**	corr_E_flag	-	Char (255)	M	C	B,S	Meta	P score	Specifies if erosion effects with respect to the reported heat-flow value were present and if corrections were performed.	[Present and corrected] [Present and not corrected] [Present not significant] [not recognized] [unspecified]	-	yes
C15	**Flag topographic effect (heat-flow correction)**	corr_TOPO_flag	-	Char (255)	M	C	B,S	Meta	P score	Specifies if topographic effects with respect to the reported heat-flow value were present and if corrections were performed.	[Present and corrected] [Present and not corrected] [Present not significant] [not recognized] [unspecified]	-	yes
C16	**Flag paleoclimatic effect (heat-flow correction)**	corr_PAL_flag	-	Char (255)	M	C	B,S	Meta	P score	Specifies if climatic conditions (glaciation, post-industrial warming, etc.) with respect to the reported heat-flow value were present and if corrections were performed.	[Present and corrected] [Present and not corrected] [Present not significant] [not recognized] [unspecified]	-	yes
C17	**Flag transient surface temperature (heat-flow correction)**	corr_SUR_flag	-	Char (255)	M	C	B,S	Meta	P score	Specifies if surface temperature variation (S) or bottom water temperature variation (B) with respect to the reported heat-flow value were present and if corrections were performed.	[Present and corrected] [Present and not corrected] [Present not significant] [not recognized] [unspecified]	-	yes
C18	**Flag convection processes (heat-flow correction)**	corr_CONV_flag	-	Char (255)	M	C	B,S	Meta	P score	Specifies if convection effects with respect to the reported heat-flow value were present and if corrections were performed.	[Present and corrected] [Present and not corrected] [Present not significant] [not recognized] [unspecified]	-	yes
C19	**Flag heat refraction effect (heat-flow correction)**	corr_HR_flag	-	Char (255)	M	C	B,S	Meta	P score	Specifies if refraction effects, e.g., due to significant local conductivity contrasts, with respect to the reported heat-flow value were present and if corrections were performed.	[Present and corrected] [Present and not corrected] [Present not significant] [not recognized] [unspecified]	-	yes
C20	**Expeditions/Platforms/Ship**	expedition	-	Char (255)	R	C	S	Meta	-	Specification of the expedition, cruise, platform or research vessel where the marine heat flow survey was conducted.	[Expedition/Cruise number] [R/V Ship] [D/V Platform] [Other (specify in comments)] [unspecified]	-	yes

. (*continued*).

ID	Field name	Short name	Unit	Field type	Obligation	Level	Domain	Group	Quality relevance	Field Description	Allowed range of values	Value description	Choice Box
C21	**Probe type**	probe_type	-	Char (255)	R	C	S	Meta	-	Type of heat-flow probe used for measurement.	[Single Steel probe (Bullard)] [Single Steel probe (Bullard) in-situ TC] [Violin-Bow probe (Lister)] [Outrigger probe (Von Herzen) in-situ TC] [Outrigger probe (autonomous) without corer] [Outrigger probe (Ewing) with corer] [Outrigger probe (autonomous) with corer] [Submersible probe] [Other (specify in comments)] [unspecified]	-	yes
C22	**Probe length**	probe_length	m	Float (2 decimal places)	R	C	S	Meta	-	Length of marine heat-flow probe.	0 – 99.99	-	no
C23	**Probe tilt**	probe_tilt	deg	Float (1 decimal place)	M	C	S	Meta	M score	Tilt of the marine heat-flow probe.	0 – 90	-	no
C24	**Bottom-water temperature**	water_temperature	°C	Float (2 decimal places)	O	C	S	Meta	-	Seafloor temperature where surface heat-flow value (q) is taken. e.g. PT 100 or Mudline temperature for ocean drilling data.	-9.99 – 999.99	-	no
C25	**Lithology**	geo_lithology	-	Char (255)	O	C	B,S	Meta	-	Dominant rock type/lithology within the interval of heat-flow determination.	= Multiple choices =	Use existing CGI simple lithology (http://resource.geosciml.org/classifier/cgi/lithology) scheme for naming the lithology.	yes
C26	**Stratigraphic age**	geo_stratigraphy	-	Char (255)	O	C	B,S	Meta	-	Stratigraphic age (series/epoch or stage/age) of the depth range involved in the reported heat-flow determination.	= Multiple choices =	Use the existing International Chronostratigraphic Chart of the International Commission on Stratigraphy (https://stratigraphy.org)	yes
C27	**Calculated or inferred temperature gradient**	T_grad_mean	K/km	Float (2 decimal places)	M	C	B,S	Temp	-	Mean temperature gradient measured for the heat-flow determination interval.	-99,999.99 – 99,999.99	-	no
C28	**Temperature gradient uncertainty**	T_grad_uncertainty	K/km	Float (2 decimal places)	R	C	B,S	Temp	-	Uncertainty (one standard deviation) of mean measured temperature gradient [T_grad_mean] as estimated by an error propagation from the uncertainty in the top and bottom temperature determinations or deviation from the linear regression of the temperature-depth data.	-99,999.99 – 99,999.99	-	no
C29	**Mean temperature gradient corrected**	T_grad_mean_cor	K/km	Float (2 decimal places)	O	C	B,S	Temp	-	Mean temperature gradient corrected for borehole (drilling/mud circulation) and environmental effects (terrain effects/topography, sedimentation, erosion, magmatic intrusions, paleoclimate, etc.). Name the correction method in the corresponding item.	-99,999.99 – 99,999.99	-	no
C30	**Corrected temperature gradient uncertainty**	T_grad_uncertainty_cor	K/km	Float (2 decimal places)	O	C	B,S	Temp	-	Uncertainty (one standard deviation) of mean corrected temperature gradient [T_grad_mean_cor] as estimated by an error propagation from the uncertainty in the top and bottom temperature determinations or deviation from the linear regression of the temperature depth data.	-99,999.99 – 99,999.99	-	no
C31	**Temperature method (top)**	T_method_top	-	Char (255)	M	C	B	Temp	M score	Method used for temperature determination at the top of the heat-flow determination interval.	[LOGeq] [LOGpert] [cLOG] [DTSeq] [DTSpert] [cDTS] [BHT] [cBHT] [DST] [cDST] [RTDeq] [RTDpert] [cRTD] [CPD] [XEN] [GTM] [BSR] [BLK] [ODTT-PC] [ODTT-TP] [SUR] [Other (specify in comments)]	[LOGeq]: continuous temperature logging in borehole equilibrium using semiconductor transducer, or thermistor probe, [LOGpert]: continuous temperature logging perturbed not n equilibrium using semiconductor transducer, or thermistor probe, [cLOG]: corrected temperature log, [DTS]: distributed temperature sensing, [DTS]: distributed temperature sensing corrected for effects, [BHT]: bottom hole temperature--uncorrected, [cBHT]: corrected bottom hole temperature, [DST]: drill stem test, [cDST]: drill stem test corrected for effects, [RTD]: resistance temperature detectors; [CPD]: Curie Point/Depth estimates, [XEN]: Xenolith, [GTM]: Geothermometry, [BSR]: bottom-simulating reflector, [BLK]: Thermal blanket, [ODTT-PC]: Ocean Drilling Temperature Tool - piston corer, [ODTT-TP]: Ocean Drilling Temperature Tool - thermistor probe, [SUR] surface temperature/bottom water temperature	yes

. (*continued*).

ID	Field name	Short name	Unit	Field type	Obligation	Level	Domain	Group	Quality relevance	Field Description	Allowed range of values	Value description	Choice Box
C32	**Temperature method (bottom)**	T_method_bottom	-	Char (255)	M	C	B	Temp	M score	Method used for temperature determination at the bottom of the heat-flow determination interval.	[LOGeq] [LOGpert] [cLOG] [DTSeq] [DTSpert] [cDTS] [BHT] [cBHT] [DST] [cDST] [RTD] [CPD] [XEN] [GTM] [BSR] [BLK] [ODTT-PC] [ODTT-TP] [Other (specify in comments)]	[LOGeq]: continuous temperature logging in borehole equilibrium using semiconductor transducer, or thermistor probe, [LOGpert]: continuous temperature logging perturbed not n equilibrium using semiconductor transducer, or thermistor probe, [cLOG]: corrected temperature log, [DTS]: distributed temperature sensing, [DTS]: distributed temperature sensing corrected for effects, [BHT]: bottom hole temperature--uncorrected, [cBHT]: corrected bottom hole temperature, [DST]: drill stem test, [cDST]: drill stem test corrected for effects, [RTD]: resistance temperature detectors; [CPD]: Curie Point/Depth estimates, [XEN]: Xenolith, [GTM]: Geothermometry, [BSR]: bottom-simulating reflector, [BLK]: Thermal blanket, [ODTT-PC]: Ocean Drilling Temperature Tool - piston corer, [ODTT-TP]: Ocean Drilling Temperature Tool - thermistor probe	yes
C33	**Shut-in time (top)**	T_shutin_top	hours	Integer (5)	R	C	B	Temp	-	Time of measurement at the interval top in relation to the end values measured during the drilling are equal to zero.	0 – 99,999	-	no
C34	**Shut-in time (bottom)**	T_shutin_bottom	hours	Integer (5)	R	C	B	Temp	-	Time of measurement at the interval bottom in relation to the end values measured during the drilling are equal to zero.	0 – 99,999	-	no
C35	**Temperature correction method (top)**	T_corr_top	-	Char (255)	R	C	B	Temp	-	Applicable only if gradient correction for borehole effects is reported. Approach applied to correct the temperature measurement for drilling perturbations at the top of the interval used for heat-flow determination.	[Horner plot] [Cylinder source method] [Line source explosion method] [Inverse numerical modelling] [Other published correction] [unspecified] [not corrected]	If you select 'Other published correction', add the author/doi to the child comment field.	yes
C36	**Temperature correction method (bottom)**	T_corr_bottom	-	Char (255)	R	C	B	Temp	-	Applicable only if gradient correction for borehole effects is reported. Approach applied to correct the temperature measurement for drilling perturbations at the bottom of the interval used for heat-flow determination.	[Horner plot] [Cylinder source method] [Line source explosion method] [Inverse numerical modelling] [Other published correction] [unspecified] [not corrected]	If you select 'Other published correction', add the author/doi to the child comment field.	yes
C37	**Number of temperature recordings**	T_number	-	Integer (6)	M	C	B,S	Temp	M score	Number of discrete temperature points (e.g. number of used BHT values, log values or thermistors used in probe sensing) confirming the mean temperature gradient [T_grad_mean_meas]. Not the repetition of one measurement at a certain depth.	0 – 999,999	-	no
C38	**Date of acquisition**	q_date	-	POSIX date (YYYY-MM)	M	C	B,S	Temp	-	The entry gives the year of the acquisition of the temperature data (which may differ from the year of publication). If the month is unknown use 01, i.e. for the year 2005 use 2005-01. For non-unique time values, define a range in the format: 'YYYY-MM; YYYY-MM'	years: 1900 – recent, months: 01– 12; [unspecified]	-	no
C39	**Mean thermal conductivity**	tc_mean	W/(mK)	Float (2 decimal place)	M	C	B,S	Cond	-	Mean conductivity in vertical direction representative for the interval of heat-flow determination. In best case, the value reflects the true in-situ conditions for the corresponding heat-flow interval.	0 – 99.99	-	no
C40	**Thermal conductivity uncertainty**	tc_uncertainty	W/(mK)	Float (2 decimal place)	R	C	B,S	Cond	-	Uncertainty (one standard deviation) of mean thermal conductivity [tc_mean]	0 – 99.99	-	no
C41	**Thermal conductivity source**	tc_source	-	Char (255)	M	C	B,S	Cond	M score	Nature of the samples upon which thermal-conductivity was determined [tc_mean].	[In-situ probe] [Core-log integration] [Core samples] [Cutting samples] [Outcrop samples] [Well-log interpretation] [Mineral computation] [Assumed from literature] [other (specify)] [unspecified]	For 'other' shortly describe the method in the child comment field.	yes
C42	**Thermal conductivity location**	tc_location	-	Char (255)	M	C	B,S	Cond	M score	Location of conductivity data used for heat-flow calculation.	[Actual heat-flow location] [Other location] [Literature/unspecified]	[literature/unspecified] only if [tc_source] = [Assumed from literature]	yes
C43	**Thermal conductivity method**	tc_method	-	Char (255)	M	C	B,S	Cond	M score	Method used for thermal-conductivity determination for [tc_mean].	[Lab - point source] [Lab - line source / full space] [Lab - line source / half space] [Lab - plane source / full space] [Lab - plane source / half space] [Lab - other] [Probe - pulse technique] [Well-log - deterministic approach] [Well-log - empirical equation] [Estimation - from chlorine content] [Estimation - from water content/porosity] [Estimation - from lithology and literature] [Estimation - from mineral composition] [unspecified]	Examples for lab devices: [Lab - point source] e.g. optical scanning TCS (thermal conductivity scanner); [Lab - line source / full space] e.g. needle probe; [Lab - line source / half space] e.g. TK04; ; [Lab - plane source / full space] e.g. hotdisc TPS, comparator apparatus, divided bar; [Lab - plane source / half space] e.g. modified TPS; For 'other' shortly describe the method in the child comment field.	yes

. (*continued*).

ID	Field name	Short name	Unit	Field type	Obligation	Level	Domain	Group	Quality relevance	Field Description	Allowed range of values	Value description	Choice Box
C44	**Thermal conductivity saturation**	tc_saturation	-	Char (255)	M	C	B,S	Cond	M score	Saturation state of the studied rock interval studied for thermal conductivity [tc_mean].	[Saturated measured in-situ] [Recovered] [Saturated measured] [Saturated calculated] [Dry measured] [other (specify)] [unspecified]	[Saturated measured insitu]: Insitu saturated measured (measurements with probe sensing / marine measurements); [Recovered]: As recovered (rocks have been preserved and measured in close to their natural saturation state); [Saturated measured]: Saturated measured (rocks have been technically saturated completely before measurement); [Saturated calculated]: Saturated calculated (thermal conductivity has been calculated from dry measured rocks, porosity and pore-filling fluid); [Dry measured]: Dry measured - rocks have been technically dried before measurement	yes
C45	**Thermal conductivity pT conditions**	tc_pT_conditions	-	Char (255)	M	C	B,S	Cond	M score	Qualified conditions of pressure and temperature under which the mean thermal conductivity [tc_mean] used for the heat-flow computation was determined.	[Unrecorded ambient pT conditions] [Recorded ambient pT conditions] [Actual in-situ (pT) conditions] [Replicated in-situ (p)] [Replicated in-situ (T)] [Replicated in-situ (pT)] [Corrected in-situ (p)] [Corrected in-situ (T)] [Corrected in-situ (pT)] [unspecified]	'Recorded' means determinations under true conditions at target depths (e.g. sensing in boreholes). 'Replicated conditions' means determinations where the conditions at target depths are replicated under laboratory conditions. 'Corrected conditions' means determinations under laboratory pT conditions that were corrected to conditions at target depths. 'Actual' means the condition at the respective depth of the heat-flow interval.	yes
C46	**Thermal conductivity pT assumed function**	tc_pT_function	-	Char (255)	R	C	B,S	Cond	-	Technique or approach used to correct the measured thermal conductivity towards in-situ pressure (p) and/or temperature (T) conditions.	[T - Tikhomirov (1968)] [T - Kutas & Gordienko (1971)] [T - Anand et al. (1973)] [T - Haenel & Zoth (1973)] [T - Blesch et al. (1983)] [T - Sekiguchi (1984)] [T - Chapman et al. (1984)] [T - Zoth & Haenel (1988)] [T - Somerton (1992)] [T - Sass et al. (1992)] [T - Funnell et al. (1996)] [T - Kukkonen et al. (1999)] [T - Seipold (2001)] [T - Vosteen & Schellschmidt (2003)] [T - Sun et al. (2017)] [T - Miranda et al. (2018)] [T - Ratcliff (1960)] [p - Bridgman (1924)] [p - Sibbitt (1975)] [p - Kukkonen et al. (1999)] [p - Seipold (2001)] [p - Durutürk et al. (2002)] [p - Demirci et al. (2004)] [p - Görgülü et al. (2008)] [p - Fuchs & Förster (2014)] [pT - Radcliff (1960)] [pT - Buntebarth (1991)] [pT - Chapman & Furlong (1992)] [pT - Emirov et al. (1997)] [pT - Abdulagatov et al. (2006)] [pT - Emirov & Ramazanova (2007)] [pT - Abdulagatova et al. (2009)] [pT - Ramazanova & Emirov (2010)] [pT - Ramazanova & Emirov (2012)] [pT - Emirov et al. (2017)] [Site-specific experimental relationships] [Other (specify in comments)] [Unspecified]	For 'other' shortly describe the method in the child comment field.	yes
C47	**Thermal conductivity number**	tc_number	-	Integer (4)	M	C	B,S	Cond	M score	Number of discrete conductivity determinations used to determine the mean thermal conductivity [tc_mean], e.g. number of rock samples with a conductivity value used, or number of thermistors used by probe sensing techniques. Not the repetition of one measurement on one rock sample or one thermistor.	0 – 9,999	-	no
C48	**Thermal conductivity averaging methodology**	tc_strategy	-	Char (255)	R	C	B,S	Cond	-	Strategy that was employed to estimate the thermal conductivity [tc_mean] over the vertical interval of heat-flow determination.	[Random or periodic depth sampling (number)] [Characterize formation conductivities] [Well log interpretation] [Computation from probe sensing] [Other] [unspecified]	For 'other' shortly describe the method in the child comment field.	yes
C49	**IGSN**	Ref_IGSN	-	Char (255)	O	C	B,S	Cond	-	International Generic Sample Numbers (IGSN, semicolon separated) for rock samples used for laboratory measurements of thermal conductivity in the heat flow calculation.	-	-	no
A1	**Reviewer_name**	Reviewer_name	-	Char (255)	A			Admin	-		= Multiple choices =	-	yes
A2	**Reviewer_comment**	Reviewer_comment	-	Char (255)	A			Admin	-		-	-	no
A3	**Review Date**	Review_date		POSIX date (YYYY-MM)	A			Admin	-		years: 1900 – recent, months: 1– 12; unclear: 99	-	no
A4	**Country**	Country	-	Char (255)	A			Admin	-		= Multiple choices =	-	yes
A5	**Region**	Region	-	Char (255)	A			Admin	-		= Multiple choices =	-	yes
A6	**Continent**	Continent	-	Char (255)	A			Admin	-		= Multiple choices =	-	yes
A7	**Domain**	Domain	-	Char (255)	A			Admin	-		= Multiple choices =	-	yes
A8	**Unique entry ID**		-	Char (255)	A			Admin	-			-	yes

. (*continued*).

Appendix B. Examples for entries of the IHFC Global Heat Flow Database

					Example:	A	B	C	D	E	F	G	G	I	J
ID	Field name	Do.	Ob.	Sc.	Unit	Probe sensing (S)					Borehole/Mine (B)				
						Location 1			Location 2		Well 1	Well 2	Well 3		
P01	Heat-flow value	B,S	M	U	mW/m²	130			109		78	63	68		
P02	Heat-flow uncertainty	B,S	M	U	mW/m²	4.8			3		3.5	1.3	5.6		
P03	Site name	B,S	M		-	location 2			location 1		well 1	well 2	well 3		
P04	Latitude (Geographical)	B,S	M		deg	40			36.8		8.5	35	53		
P05	Longitude (Geographical)	B,S	M		deg	-20			16		114.2	13	120		
P06	Elevation (Geographical)	B,S	M	M	m	0			0				0		
P07	Basic geographical environment	B,S	M		-	Offshore (marine)			Offshore (marine)		Onshore (continental)	Onshore (continental)	Onshore (continental)		
P08	General comments parent level	B,S	R		-										
P09	Flag heat production of the overburden	B,S	R		-	No			No		Yes	No	Yes		
P10	Total measured depth	B	R		m						800	1500	2500		
P11	Total true vertical depth	B	R								750	1300	2448		
P12	Type of exploration method	B	M		-	mapping			mapping		drilling	drilling	drilling		
P13	Original exploration purpose	B	R		-	hydrocarbon			hydrocarbon		geothermal	groundwater	geothermal		
C01	Heat-flow value child	B,S	M	U	mW/m²	135	126	129	109	119	78	63	60	67	77
C02	Heat-flow uncertainty child	B,S	M	U	mW/m²	5.6	3.9	4.9	3	4	3.5	1.3	3	7	6.8
C03	Heat-flow method	B,S	M		-	Bullard	Bullard	Bullard	Bullard	Bullard	Fourier	Fourier	Fourier	Fourier	Fourier
C04	Heat-flow interval top	B,S	M	M	m	0	0	0	0	0	500	1230	750	1205	2100
C05	Heat-flow interval bottom	B	M	M	m						650	1235	780	1230	2300
C06	Penetration depth	S	M	M	m	2.3	6.5	1.9	11.2	4.6	-	-	-	-	-
C07	Primary publication reference	B,S	M		-	Alber4_1979	Alber4_1979	Beltran5_1979	Test2_1979	Doe3_1979	Test1_etal._2020	Doe2_etal._2021	Afand3_etal._2021	Afand3_etal._2021	Afand3_etal._2021
C08	Primary data reference	B,S	R		-										
C09	Relevant child	B,S	M		-	Yes	No	No	Yes	Yes	Yes	Yes	Yes	No	Yes
C10	General comments child level	B,S	R		-										
C11	Flag in-situ thermal properties	B,S	R		-	Corrected – pT	not corrected	not corrected	Corrected – pT	Corrected – pT	Corrected – pT	not corrected	Corrected – T	not corrected	Corrected – T
C12	Flag temperature corrections	B,S	M	M	-	not corrected	not corrected	not corrected	Tilt corrected	Drift corrected	unspecified	unspecified	unspecified	unspecified	unspecified
C13	Flag sedimentation effect	B,S	M	P	-	Present and	Present and	Present and	Present and	Present and	unspecified	Present and	unspecified	Present and	unspecified
C14	Flag erosion effect	B,S	M	P	-	not recognized	not recognized	not recognized	not recognized	not recognized	unspecified	not recognized	unspecified	Present and	unspecified
C15	Flag topographic effect	B,S	M	P	-	not recognized	not recognized	not recognized	not recognized	not recognized	unspecified	not recognized	unspecified	Present and	unspecified
C16	Flag paleoclimatic effect	B,S	M	P	-	not recognized	not recognized	not recognized	not recognized	not recognized	unspecified	unspecified	unspecified	Present and	unspecified
C17	Flag surface / bottom water temperature	B,S	M	P	-	Present and corrected	Present and corrected	Present and corrected	Present and corrected	Present and corrected	unspecified	unspecified	unspecified	unspecified	unspecified
C18	Flag convection processes	B,S	M	P	-	not recognized	not recognized	not recognized	Present and	not recognized	unspecified	unspecified	unspecified	unspecified	unspecified
C19	Flag heat refraction effect	B,S	M	P	-	Present and	Present and	Present and	Present and	Present and	unspecified	Present and	unspecified	Present and	unspecified
C20	Expeditions/Platforms/Ship	B,S	R		-	Cruise 3	Cruise 3	Cruise 3	Cruise 1	Cruise 2					
C21	Probe type	S	R		-	Outrigger probe (Ewing) with corer	Outrigger probe (Von Herzen) with corer	Outrigger probe (autonomous) with corer	Single Steel probe (Bullard)	Outrigger probe (Ewing) without corer	-	-	-	-	-
C22	Probe length	S	R		m	6	6	6	7.8	5					
C23	Probe tilt	S	M	M	deg	3	2.8	15	8.7	14					
C24	Bottom-water temperature	S	O		°C	1.8	1.8	1.8	1.3	2.8					
C25	Lithology	B,S	O		-	Sediment	Sediment	Sediment	Sediment	Sediment	sandstone	carbonate	silty sandstones	limestone	tuff; sand; volcanic breccia; sulfur
C26	Stratigraphic age	B,S	O		-	Cenozoic	Cenozoic	Cenozoic	Cenozoic	Cenozoic	Jurassic	Triassic	Holocene	Holocene	Permian
C27	Calculated or inferred temperature gradient	B,S	M		K/km	85	93	62	78	120	28	33	41	38	25
C28	Temperature gradient uncertainty	B,S	R		K/km	5	4.8	2.9	0.05	1.3	1.2	0.8	1.9	3.5	5
C29	Mean temperature gradient corrected	B,S	O		K/km										
C30	Corrected temperature gradient uncertainty	B,S	O		K/km										
C31	Temperature method (top)	B	M	M	-						Sur	LOGpert	Logeq	BHT	DTSpert
C32	Temperature method (bottom)	B	M	M	-						BHT	LOGpert	Logeq	CPD	DTSpert
C33	Shut-in time (top)	B	R		hr										
C34	Shut-in time (bottom)	B	R		hr										
C35	Temperature correction method (top)	B	R		-							Cylinder source method			
C36	Temperature correction method (bottom)	B	R		-						Horner plot	Cylinder source method			
C37	Number of temperature recordings	B,S	M	M	-	7	5	11	3	5	1	26	120	2	15
C38	Date of acquisition	B,S	M		YYYY-MM						1999	1999-01			
C39	Mean thermal conductivity	B,S	M		W/(mK)	1.59	1.35	2.08	1.15	0.91	2.79	1.91	1.46	1.76	3.08
C40	Thermal conductivity uncertainty	B,S	R		W/(mK)										
C41	Thermal conductivity source	B,S	M	M	-	In-situ probe	In-situ probe	In-situ probe	In-situ probe	In-situ probe	Core-log integration	Core samples	Cutting samples	Core samples	Mineral computation
C42	Thermal conductivity location	B,S	M	M		Actual heat-flow location	Actual heat-flow location	Other location	Actual heat-flow location	Actual heat-flow location	Actual heat-flow location	Actual heat-flow location	Actual heat-flow location	Actual heat-flow location	Actual heat-flow location
C43	Thermal conductivity method	B,S	M	M-score (S)	-	Probe - pulse technique	Probe - pulse technique	Probe - pulse technique	Probe - pulse technique	Probe - pulse technique	Lab - point source	Lab - line source / half space	Well-log - deterministic approach	Well-log - empirical equation	Estimation - from lithology and literature
C44	Thermal conductivity saturation	B,S	M	M	-	Recovered	Recovered	Recovered	Recovered	Recovered	Saturated measured insitu	Saturated calculated	Saturated measured	Dry measured	Saturated measured
C45	Thermal conductivity pT conditions	B,S	M	M	-	Corrected in-situ (pT)	Unspecified	Unspecified	Corrected in-situ (pT)	Corrected in-situ (pT)	Corrected in-situ (pT)	Unspecified	Replicated in-situ (T)	Unspecified	Unspecified
C46	Thermal conductivity pT assumed function	B,S	R		-	pT - Radcliff (1960)			pT - Radcliff (1960)	pT - Radcliff (1960)					
C47	Thermal conductivity number	B,S	M	M	-	5	5	5	5	5	5	10	5	5	5
C48	Thermal conductivity averaging methodology	B,S	R		-	Unspecified	Unspecified	Unspecified	Unspecified	Unspecified	Random or periodic depth sampling (number)	Characterize formation conductivities	Random or periodic depth sampling (number)	Random or periodic depth sampling (number)	Random or periodic depth sampling (number)
C49	IGSN	B,S	O		-										

References

Alföldi, L., Galfi, J., Liebe, P., 1985. Heat flow anomalies caused by water circulation. J. Geodyn. 4 (1–4), 199–217. https://doi.org/10.1016/0264-3707(85)90060-2.

Badro, J., Rueff, J.P., Vanko, G., Monaco, G., Fiquet, G., Guyot, F., 2004. Electronic transitions in perovskite: possible non-convecting layers in the lower mantle. Science 305 (5682), 383–386. https://doi.org/10.1126/science.1098840.

Balling, N., Haenel, R., Ungemach, P., Vasseur, G., Wheildon, J., 1981. Preliminary Guidelines for Heat Flow Density Determination. Commission of the European Communities, p. 31.

Beardsmore, G.R., Cull, J.P., 2001. Crustal Heat Flow: A Guide to Measurement and Modelling. University Press, Cambridge.

Beck, A.E., Balling, N., 1988. Determination of virgin rock temperatures. In: Haenel, R., Rybach, L., Stegena, L. (Eds.), Handbook of Terrestrial Heat-Flow Density Determination. Kluwer Academic Publishers, Dordrecht, pp. 59–85.

Bédard, K., Comeau, F.-A., Raymond, J., Malo, M., Nasr, M., 2017. Geothermal characterization of the St. Lawrence Lowlands Sedimentary Basin, Québec, Canada. Nat. Resour. Res. 2017, 1–24. https://doi.org/10.1007/s11053-017-9363-2.

Birch, F., 1954. Heat from Radioactivity, New York.

Blackwell, D.D., Steele, J.L., Carter, L.S., 1991. Heat flow patterns of the North American continent: A discussion of the DNAG geothermal map of North America, pp. 423–437. In: Slemmons, D.B., Engdahl, E.R., Blackwell, D.D. (Eds.), Neotectonics of North America, Geological Society of America. DNAG Decade Map Volume 1, p. 498.

Bodri, L., Cermak, V., 2007. Borehole climatology. A new method on how to reconstruct climate, Elsevier, Amsterdam, p. 335.

Boyd, F.R., 1973. A pyroxene geotherm. Geochim. Cosmochim. Acta 37, 2533–2546. https://doi.org/10.1016/0016-7037(73)90263-9.

Bullard, E.C., 1939. Heat flow in South Africa. Proc. Royal Soc. London. Series A. Math. Phys. Sci. 173 (955), 474–502. https://doi.org/10.1098/rspa.1939.0159.

Bullard, E.C., 1954. The flow of heat through the floor of the Atlantic Ocean. Proc. Royal Soc. London. Series A. Math. Phys. Sci. 222 (1150), 408–429. https://doi.org/10.1098/rspa.1954.0085.

Carlino, S., 2018. Heat flow and geotemperature gradients of the Campania region (Southern Italy) and their relationship to volcanism and tectonics. J. Volcanol. Geotherm. Res. 365, 23–37. https://doi.org/10.1016/j.jvolgeores.2018.10.015.

Čermák, V., Rybach, L. (Eds.), 1979. Terrestrial Heat Flow in Europe. Springer Verlag, Heidelberg-Berlin-New York, p. 328. ISBN 3–540–09440-7.

Čermák, V., Rybach, L. (Eds.), 1991. Terrestrial Heat Flow and the Lithosphere Structure. Springer-Verlag, Berlin and Heidelberg, p. 507.

Chapman, D.S., Pollack, H.N., 1975. Global heat flow: a new look. Earth Planet. Sci. Lett. 28, 23–32. https://doi.org/10.1016/0012-821X(75)90069-2.

Chapman, D.S., Rybach, L., 1985. Heat flow anomalies and their interpretation. J. Geodyn. 4 (1–4), 3–37. https://doi.org/10.1016/0264-3707(85)90049-3.

Clauser, C., 2006. Geothermal energy. In: Heinloth, K. (Ed.), Landolt-Börnstein, Group VIII: Advanced Materials and Technology, Energy Technologies, Subvol, vol. 3. C Renewable Energies, Springer Verlag, Heidelberg-Berlin, pp. 493–604.

Davies, J.H., 2013. Global map of solid Earth surface heat flow. Geochem. Geophys. Geosyst. 14 (10), 4608–4622. https://doi.org/10.1002/ggge.20271.

Davies, J.H., Davies, D.R., 2010. Earth's surface heat flux. Solid Earth 1 (1), 5–24. https://doi.org/10.5194/se-1-5-2010.

Davis, E.E., Villinger, H., MacDonald, R.D., et al., 1997. A robust rapid-response probe for measuring bottom-hole temperatures in Deep-Ocean Boreholes. Mar. Geophys. Res. 19, 267–281. https://doi.org/10.1023/A:1004292930361.

Desonie, D., 2008. Polar Regions: Human Impacts. Chelsea House, New York.

Förster, A., 2001. Analysis of borehole temperature data in the Northeast German Basin: continuous logs versus bottom-hole temperatures. Pet. Geosci. 7 (3), 241–254. https://doi.org/10.1144/petgeo.7.3.241.

Freifeld, B.M., Finsterle, S., Onstott, T.C., Toole, P., Pratt, L.M., 2008. Ground surface temperature reconstructions: using in situ estimates for thermal conductivity acquired with a fiber-optic distributed thermal perturbation sensor. Geophys. Res. Lett. 35, L14309. https://doi.org/10.1029/2008GL034762.

Fuchs, S., Beardsmore, G., Chiozzi, P., Espinoza-Ojeda, O.M., Gola, G., Gosnold, W., Harris, R., Jennings, S., Liu, S., Negrete-Aranda, R., Neumann, F., Norden, B., Poort, J., Rajver, D., Ray, L., Richards, M., Smith, J.D., Tanaka, A., Verdoya, M., 2021a. A new database structure for the IHFC Global Heat Flow Database. Int. J. Terrestrial Heat Flow Appl. 4, 1, 1–14. https://doi.org/10.31214/ijthfa.v4i1.62.

Fuchs, S., Norden, B., International Heat Flow Commission, 2021b. The Global Heat Flow Database: Release 2021. GFZ Data Services. https://doi.org/10.5880/fidgeo.2021.014.

Furlong, K.P., Chapman, D.S., 2013. Heat flow, heat generation, and the thermal state of the lithosphere. Annu. Rev. Earth Planet. Sci. 41, 385–410. https://doi.org/10.1146/annurev.earth.031208.100051.

Gasparini, P., Mantovani, M.S.M., Corrado, G., Rapolla, A., 1979. Depth of Curie temperature in continental shields: a compositional boundary? Nature 278, 845–846. https://doi.org/10.1038/278845a0.

Gerard, R., Langseth, M.G., Ewing, M., 1962. Temperature gradient measurements in the water and bottom sediment of the western Atlantic. J. Geophys. Res. 67 (2), 785–803. https://doi.org/10.1029/JZ067i002p00785.

Global Heat Flow Compilation Group, 2013. Component parts of the World Heat Flow Data Collection. PANGAEA. https://doi.org/10.1594/PANGAEA.810104.

Global Heat Flow Data Assessment Group et al, 2023. The Global Heat Flow Database: Update 2023, V. 1. Services, GFZ Data. https://doi.org/10.5880/fidgeo.2023.008.

Gosnold, W., Njoku, G., 2017. Heat flow and climate change. GRC Trans. 41, 1892–1907.

Haenel, R., 1979. A critical review of heat flow measurements in Sea and lake bottom sediments. In: Cermak, V., Rybach, L. (Eds.), Terrestrial Heat Flow in Europe. Springer-Verlag, Berlin, pp. 49–73.

Haenel, R., Rybach, L., Stegena, L., 1988. Handbook of Terrestrial Heat-Flow Density Determination, vol. 4. Kluwer Academic Publishers, Dordrecht.

Harris, R.N., Chapman, D.S., 2001. Mid-latitude (30°–60° N) climatic warming inferred by combining borehole temperatures with surface air temperatures. Geophys. Res. Lett. 28 (5), 747–750. https://doi.org/10.1029/2000GL012348.

Harris, R.N., Spinelli, G.A., Hutnak, M., 2020. Heat Flow evidence for hydrothermal circulation in oceanic crust offshore Grays Harbor, Washington. Geochem. Geophys. Geosyst. 21 (6), 1–20. https://doi.org/10.1029/2019GC008879.

Hasterok, 2019. ThermoGlobe: an Online Global Heat Flow Database online: http://heatflow.org, last accessed 02/2023.

Heesemann, M., Villinger, H., Fisher, A.T., Tréhu, A.M., White, S., 2006. Data report: testing and deployment of the new APCT-3 tool to determine in situ temperatures while piston coring. In: Riedel, M., Collett, T.S., Malone, M.J. (Eds.), and the Expedition 311 Scientists. *Proc. IODP,* 311: Washington, DC (Integrated Ocean Drilling Program Management International, Inc.). https://doi.org/10.2204/iodp.proc.311.108.2006.

Houseman, G.A., Cull, J.P., Muir, P.M., Paterson, H.L., 1989. Geothermal signatures and uranium deposits on the Stuart Shelf of South Australia. Geophysics 54 (2), 158–170. https://doi.org/10.1190/1.1442640.

Huang, S., Pollack, H.N., Shen, P.Y., 2000. Temperature trends over the past five centuries reconstructed from borehole temperatures. Nature 403 (6771), 756–758. https://doi.org/10.1038/35001556.

Hunt, C.P., Moskowitz, B.M., Banerjee, S.K., 1995. Magnetic properties of rocks and minerals. In: Ahrens, T.J. (Ed.), Rock Physics and Phase Relations: A Handbook of Physical Constants. American Geophysical Union, Washington, D. C, pp. 189–204. https://doi.org/10.1029/RF003p0189.

Jemsek, J., Von Herzen, R., Andrew, P., 1985. In-Situ Measurement of Thermal Conductivity Using the Continuous-Heating Line-Source Method and WHOI Outrigged Probe. Technical report, Woods Hole Oceanographic Institution.

Jessop, A.M., Hobart, M.A., Sclater, J.G., 1976. The World Heat Flow Data Collection - 1975. Geological survey of Canada, Earth Physics Branch, Geothermal Series, 5, p. 10 doi:10013/epic.40176.d002.

Jiang, G., Hu, S., Shi, Y., Zhang, C., Wang, Z., Hu, D., 2019. Terrestrial heat flow of continental China: Updated dataset and tectonic implications. Tectonophysics 753, 36–48. https://doi.org/10.1016/j.tecto.2019.01.006.

Johnson, P., Hutnak, M., 1997. Conductive heat loss in recent eruptions at mid-ocean ridges. Geophys. Res. Lett. 24 (23), 3089–3092. https://doi.org/10.1029/97GL02998.

Kukkonen, I.T., Peltonen, P., 1999. Xenolith-controlled geotherm for the central Fennoscandian Shield: implications for lithosphere-asthenosphere relations. Tectonophysics 304, 301–315. https://doi.org/10.1016/S0040-1951(99)00031-1.

Le Gal, V., Lucazeau, F., Cannat, M., Poort, J., Monnin, C., Battani, A., Fontaine, F., Goutorbe, B., Rolandone, F., Poitou, C., Blanc-Valleron, M.-M., Piedade, A., Hipólito, A., 2018. Heat flow, morphology, pore fluids and hydrothermal circulation in atypical Mid-Atlantic Ridge flank near Oceanographer Fracture Zone. Earth Planet. Sci. Lett. 482, 423–433. https://doi.org/10.1016/j.epsl.2017.11.035.

Lee, W.H.K., 1963. Heat flow data analysis. Rev. Geophys. 1 (3), 449–479. https://doi.org/10.1029/RG001i003p00449.

Lee, W.H.K., Clark, S.P., 1966. Heat flow and volcanic temperatures. In: Clark, S.P. (Ed.), Handbook of Physical Constants, vol. 97. Geological Society of America memoir, New York, pp. 487–511.

Lee, W.H.K., Uyeda, S., 1965. Review of heat flow data. In: Terrestrial Heat Flow. American Geophysical Union, pp. 87–190. https://doi.org/10.1029/GM008p0087.

Lister, C.R.B., 1979. The pulse-probe method of conductivity measurement. Geophys. J. Int. 57 (2), 451–461. https://doi.org/10.1111/j.1365-246X.1979.tb04788.x.

Lotz, B., 2004. Neubewertung des rezenten Wärmestroms im Nordostdeutschen Becken. Thesis, p. 228. http://dx.doi.org/10.17169/refubium-8397.

Louden, K.E., Wright, J.A., 1989. Marine heat flow data: A new compilation of observations and brief review of its analysis. In: Wright, J.A., Louden, K.E. (Eds.), CRC Handbook of Seafloor Heat flow. CRC Press, Boca Raton, FL, pp. 3–72.

Lucazeau, F., 2019. Analysis and Mapping of an Updated Terrestrial Heat Flow Data Set. Geochem. Geophys. Geosyst. 20 (8), 4001–4024. https://doi.org/10.1029/2019gc008389.

Majorowicz, J.A., Gough, D.I., Lewis, T.J., 1993. Correlation between the depth to the lower-crustal high conductive layer and heat flow in the Canadian Cordillera. Tectonophysics 225, 49–56. https://doi.org/10.1016/0040-1951(93)90247-H.

Mareschal, J.C., Jaupart, C., 2013. Radiogenic heat production, thermal regime and evolution of continental crust. Tectonophysics 609, 524–534. https://doi.org/10.1016/j.tecto.2012.12.001.

Nielsen, S.B., Balling, N., Christiansen, H.S., 1990. Formation temperatures determined from stochastic inversion of borehole observations. Geophys. J. Int. 101, 581–591. https://doi.org/10.1111/j.1365-246X.1990.tb05572.x.

Osterkamp, T.E., Burn, C.R., 2003. Permafrost. In: North, G.R., Pyle, J.A., Zhang, F. (Eds.), Encyclopedia of Atmospheric Sciences, vol. 4. Elsevier, pp. 1717–1729 (ISBN 978-0-12-382226-0.).

Pascal, C., 2015. Heat flow of Norway and its continental shelf. Mar. Pet. Geol. 66, 956–969. https://doi.org/10.1016/j.marpetgeo.2015.08.006.

Pauselli, C., Gola, G., Mancinelli, P., Trumpy, E., Saccone, M., Manzella, A., Ranalli, G., 2019. A new surface heat flow map of the Northern Apennines between latitudes 42.5 and 44.5 N. Geothermics 81, 39–52. https://doi.org/10.1016/j.geothermics.2019.04.002.

Pollack, N.H., 1982. The Heat Flow from the Continents. Annu. Rev. Earth Planet. Sci. 10, 459–481. https://doi.org/10.1146/annurev.ea.10.050182.002331.

Polyak, B.G., Khutorskoy, M.D., 2018. Heat flow from the Earth interior as indicator of deep processes. Georesources 20 (4), 366–376. https://doi.org/10.18599/grs.2018.4.366-376.

Powell, W.G., Chapman, D.S., Balling, N., Beck, A.E., 1988. Continental heat-flow density. In: Haenel, R., Rybach, L., Stegena, L. (Eds.), Handbook of Terrestrial Heat-Flow Density Determination. Kluwer Academic Publishers, Dordrecht, pp. 167–222.

Pribnow, D., Kinoshita, M., Stein, C., 2000. Thermal Data Collection and Heat Flow Recalculations for ODP Legs 101–180. Inst. for Jt. Geosci. Res, GGA, Hannover, Germany.

Richards, M., Blackwell, D.D., Williams, M., Frone, Z., Dingwall, R., Batir, J., Chickering, C., 2012. Proposed Reliability Code for Heat Flow Sites. GRC Trans. 36, 211–217.

Ritter, U., Zielinski, G.W., Weiss, H.M., Zielinski, R.L.B., Sættem, J., 2004. Heat flow in the Vøring Basin, mid. Norwegian shelf. Pet. Geosci. 10, 353–365. https://doi.org/10.1144/1354-079303-616.

Sass, J., Lachenbruch, A., 1979. Thermal regime of the Australian continental crust. In: McElhinny, M.W. (Ed.), The Earth — Its Origin, Structure and Evolution. Academic, London, pp. 301–351.

Schumacher, S., Moeck, I., 2020. A new method for correcting temperature log profiles in low-enthalpy plays. Geotherm Energy 8, 27. https://doi.org/10.1186/s40517-020-00181-w.

Sclater, J.G., Crowe, J., 1979. A heat flow survey at anomaly 13 on the Reykjanes Ridge: a critical test of the relation between heat flow and age. J. Geophys. Res. 84 (B4), 1593–1602. https://doi.org/10.1029/JB084iB04p01593.

Shapiro, N.M., Ritzwoller, M.H., 2004. Inferring surface heat flux distributions guided by a global seismic model: particular application to Antarctica. Earth Planet. Sci. Lett. 223, 213–224. https://doi.org/10.1016/j.epsl.2004.04.011.

Simmons, G., Horai, K.-I., 1968. Heat flow data. 2. J. Geophys. Res. (1896–1977) 73 (20), 6608–6609. https://doi.org/10.1029/JB073i020p06608.

Swanberg, C.A., Morgan, P., 1979. The linear relation between temperatures based on the silica content of groundwater and regional heat flow: a new heat flow map of the United States. In: Rybach, L., Stegena, L. (Eds.), Geothermics and Geothermal Energy. Contributions to Current Research in Geophysics (CCRG). Birkhäuser, Basel. https://doi.org/10.1007/978-3-0348-6525-8_20.

Tanaka, A., Okubo, Y., Matsubayashi, O., 1999. Curie point depth based on spectrum analysis of the magnetic anomaly data in East and Southeast Asia. Tectonophysics 306, 461–470. https://doi.org/10.1016/S0040-1951(99)00072-4.

Taylor, J.R., 1997. An Introduction to Error Analysis: The Study of Uncertainties in Physical Measurements, Univ. Science, Sausalito, CA, 45, p. 92.

Turcotte, D.L., Schubert, G., 2002. Geodynamics, 2nd ed. Cambridge University Press, Cambridge, New York, Melbourne, p. xv 456.

Wang, K., Lewis, T.J., 1992. Geothermal evidence from Canada for a cold period before recent climatic warming. Science 256, 1002–1005. https://doi.org/10.1126/sciadv.abg9551.

White, R.S., 1979. Gas hydrate layers trapping free gas in the Gulf of Oman. Earth Planet. Sci. Lett. 42 (1), 114–120. https://doi.org/10.1016/0012-821X(79)90196-1.

Yamano, M., Uyeda, S., Aoki, Y., Shipley, T.H., 1982. Estimates of heat flow derived from gas hydrates. Geology 10 (7), 339–343. https://doi.org/10.1130/0091-7613(1982)10<339:EOHFDF>2.0.CO;2.